Available online at www.sciencedirect.com

ScienceDirect

Green Energy & Environment 2 (2017) 331−362

www.keaipublishing.com/gee

Review article

A review on photoelectrochemical cathodic protection semiconductor thin films for metals

Yuyu Bu, Jin-Ping Ao*

Institute of Technology and Science, Tokushima University, 2-1 Minami-Josanjima, Tokushima 770-8506, Japan

Received 26 December 2016; revised 8 February 2017; accepted 8 February 2017
Available online 15 February 2017

Abstract

Photoelectrochemical (PEC) cathodic protection is considered as an environment friendly method for metals anticorrosion. In this technology, a n-type semiconductor photoanode provides the photogenerated electrons for metal to achieve cathodic protection. Comparing with traditional PEC photoanode for water splitting, it requires the photoanode providing a suitable cathodic potential for the metal, instead of pursuit ultimate photon to electric conversion efficiency, thus it is a more possible PEC technology for engineering application. To date, great efforts have been devoted to developing novel n-type semiconductors and advanced modification method to improve the performance on PEC cathodic protection metals. Herein, recent progresses in this field are summarized. We highlight the fabrication process of PEC cathodic protection thin film, various nanostructure controlling, doping, compositing methods and their operation mechanism. Finally, the current challenges and future potential works on improving the PEC cathodic protection performance are discussed.
© 2017, Institute of Process Engineering, Chinese Academy of Sciences. Publishing services by Elsevier B.V. on behalf of KeAi Communications Co., Ltd. This is an open access article under the CC BY-NC-ND license (http://creativecommons.org/licenses/by-nc-nd/4.0/).

Keywords: Photoelectrochemical cathodic protection; TiO_2 photoanode; $SrTiO_3$; g-C_3N_4; Photo-electron storage

1. Introduction

Metal corrosion is a quiet destruction. The most of metals in nature have a trend of transforming to oxides or stable compounds, except Au, Pt and other noble metals. Therefore there are very few pure metals in the nature. Engineering metal materials (such as Fe, Al, Cu, Mg, etc.) which extracted from ore or oxide posses strong tendency of returning to a stable state. This phenomenon that the metal changes back to its metal compound and loses the original metal characteristics in surrounding environmental (such as moisture, temperature, acid, alkali, salt and other chemical substances, etc.), is considered as corrosion. According to the statistics, China's annual economic losses caused by metal corrosions account for 1.5−3% of the GDP [1]. The specific hazards induced by metal corrosion are shown in Fig. 1-1, including materials wasting, environment pollution caused by the metal ions dissolution and serous engineering safety accidents caused by corrosion.

Cathodic protection is one of the most widely applied technologies for engineering metal anticorrosion. It can be classified into two types: impressed current cathodic protection and sacrificial anode protection. The impressed current cathodic protection is that the protected metal will ohmic connect with the negative pole of the external power source, and an inert electrode will connect with the positive pole. Both of them are placed in the corrosion electrolyte to form an electrolytic cell, thus the metal will be protected as a cathode. This method is mainly employed to protect metals that used in the soil, sea water and river which can provide an electrolytic cell environment. The sacrificial anodic protection is that connect a piece of active metal (Zinc is the most widely used metal) with a much more negative self-corrosion potential than the protected metal, attributing to

* Corresponding author.
E-mail address: jpao@ee.tokushima-u.ac.jp (J.-P. Ao).

http://dx.doi.org/10.1016/j.gee.2017.02.003
2468-0257/© 2017, Institute of Process Engineering, Chinese Academy of Sciences. Publishing services by Elsevier B.V. on behalf of KeAi Communications Co., Ltd. This is an open access article under the CC BY-NC-ND license (http://creativecommons.org/licenses/by-nc-nd/4.0/).

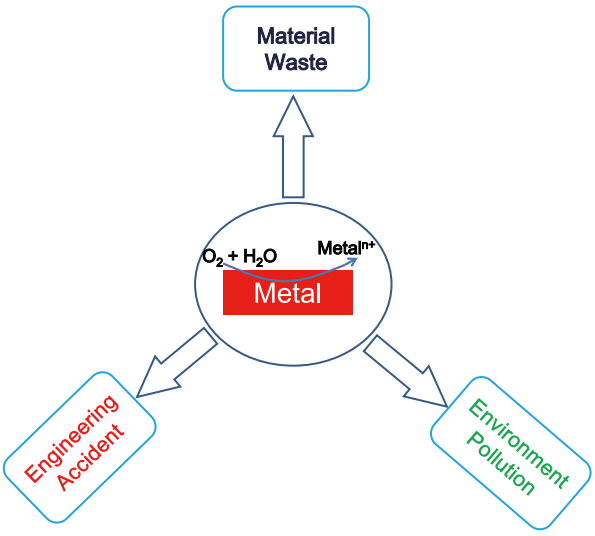

Fig. 1-1. The harms of the metal corrosion.

the self-corrosion potential difference between them, the protected metal can be polarized to the corrosion stable region by the sacrificial metal anode [2].

At present, although the cathodic protection technology has been widely used in the area of metal anticorrosion, it also has some shortcomings, such as electric energy wasting, sacrificial anode wasting and environmental pollution. Today, under the background of energy shortage and environment pollution, developing some green, non-polluting new energy conversion technologies and applying them on the field of metal cathodic protection are very emergency [3,4].

Photoelectrochemical (PEC) cathodic protection technology is a new, green, non-polluting metal cathodic protection method. The protection model is shown in Fig. 1-2. It is well known that the primary cause of metal corrosion is the presence of oxidizing species [5] in the corrosive medium, whose redox potential should be more positive than the self-corrosion

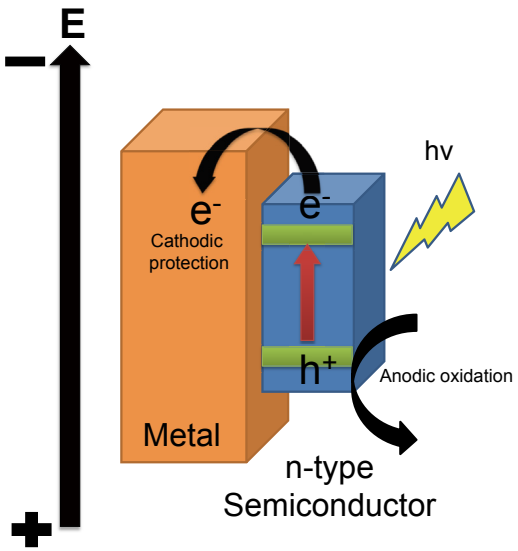

Fig. 1-2. The model of PEC cathodic protection for metal by photoanode.

potential of the metal. The essence of the cathodic protection is providing a more negative electron to the protected metal, which can be oxidized by the oxidizing species, to replace the metal corrosion. If the transfer rate of the photogenerated electrons to the metal is higher than that of the electrons consuming speed during the metal oxidation process, the photogenerated electrons will be enriched in the protected metal, and polarize the potential of the metal to a more negative region. According to the above principle of cathodic protection, it is believed that the semiconductor PEC cathodic protection is feasible, but the physical and chemical characterizations of the semiconductor material have special requirements: (1) The conduction band (CB) potential of semiconductor must be more negative than the self-corrosion potential of protected metal. In this case, the photogenerated electrons can stride the energy barrier between the semiconductor and the protected metal, and replace the metal to become the cathode for the oxidizing species in the corrosive medium; (2) The semiconductors must be in a n-type rectifying effect. In the metal cathodic protection process, the protected metal electrode must be used as the cathode and the semiconductor electrode serve as anode. We know that a photoanode current can be obtained on a n-type semiconductor thin film photoelectrode under the illumination. Therefore, based on the n-type rectifying effect, the photoanode can be used to provide photogenerated electrons to the metal for protecting it. However, the rectifying effect of p-type semiconductor is contrary to the n-type one, so it is not suitable for PEC cathodic protection; (3) Photogenerated holes must be trapped by hole-trapping agent. In photoanode, the photogenerated electrons transfer speed is much faster than the photogenerated holes, so electrons can arrive the back substrate rapidly through the semiconductor thin film, and then transfer to the protected metal. Meanwhile, the photogenerated hole will transfer to the surface of the semiconductor, and oxidize hole-trapping agents surrounding it. However, if there is no hole-trapping agent in the environment medium or the content of the agent is very low, the anode depolarization process will be inhibited, which will increase the difficulty of separation process of the photogenerated electron–hole pairs. In general, the water molecules in the environment medium present widely. Therefore the potential of photogenerated holes produced by photoanode should be more positive than the water oxidation potential; (4) Semiconductor materials must be stable, which cannot be corroded by the surrounding environment medium in the protection process [6].

The photogenerated electrons transfer mechanism during the PEC cathodic protection process is shown in Fig. 1-3 (Taking the PEC protection system of the TiO_2 in NaCl electrolyte photoelectrode on the 304 SS as a example). Fig. 1-3A shows the state of energy band potential of TiO_2 photoanode, 304 SS and NaCl photoelectrolyte before reaching equilibration. $E_{304\ SS}$ is the corrosion potential of 304 SS in 3.5 wt% NaCl solution, which is more positive than the E_{Fermi} of the n-type TiO_2 semiconductor. E_{NaCl/H_2O} is the oxidation-reduction potential of the 3.5 wt% NaCl electrolyte, which is more positive than $E_{304\ SS}$. When the semiconductor

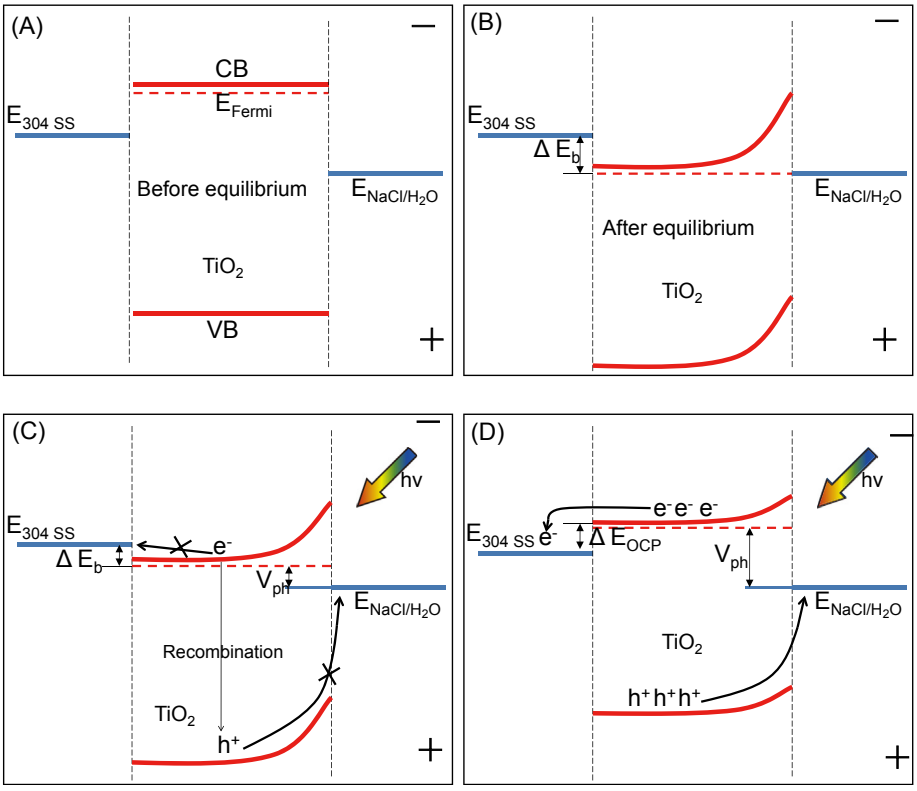

Fig. 1-3. Mechanism for PEC cathodic protect 304 SS by TiO_2 photoanodes. (A) Before system equilibrium; (B) After the system equilibrium; (C) The situation of the system after light illuminate the low-efficiency photoanode; (D) The situation of the system after light illuminate the high-efficiency photoanode.

electrode was immersed into the electrolyte, the Fermi level would be pulled to the oxidation-reduction potential of the electrolyte (Fig. 1-3B). Therefore an upward bend will be formed at the interface between the semiconductor and the electrolyte. The energy band which is far from the interface, shifts positive direction. In this case, E_{Fermi} is more positive than the self-corrosion potential of $E_{304\ SS}$, an electron transfer barrier ΔE_b is formed between them. When the semiconductor is excited by the incident light (Fig. 1-3C), the electrons are excited from the valence band to the CB (CB), and the E_{Fermi} is shifted negatively again to form the photovoltage V_{ph}. The magnitude of V_{ph} depends on the flat band potential of the semiconductor and the amount of free photogenerated electrons on the CB after excitation by the incident light. If the separation ability of photoelectrons and holes of the TiO_2 photoanode is weak, it will induce the value of V_{ph} too small. In this case, the E_{Fermi} potential of the semiconductor cannot move to more negative region than the $E_{304\ SS}$ potential after photo excitation. Thus, a PEC cathodic protection cannot be formed on 304 SS. On the contrary, as shown in Fig. 1-3D, if the TiO_2 photoanode has a strong separation ability of photogenerated electrons and holes, the number of excited free electrons on the CB will be increased and a larger V_{ph} can be achieved, resulting in a more negative E_{Fermi} than $E_{304\ SS}$. At this time, the photogenerated electrons can transfer from the CB of TiO_2 to 304 SS and form a cathodic protection. The cathodic protection potential drop (ΔE_{OCP}) is shown in Fig. 1-3D [7,8].

Except environment friendly, PEC cathodic protection technology is also possessing strong background for engineering application. First of all, some research results have showed that solar radiation, especially the component of UV has an important impact on the metal corrosion process by metal corrosion products such as Fe_2O_3, FeOOH, ZnO, CuO, Cu_2O and other semiconducting substances [9–12]. When exposing them to sunlight, due to the photovoltaic effect of them, the separated photogenerated electrons and holes would be produced. Because the CB potentials of these semiconductors are generally more positive than their corresponding self-corrosion potential of metals, the photogenerated electrons cannot participate in the metal cathode reaction process. On the contrary, the photogenerated holes with strong oxidizing ability, which can participate in and accelerate the process of metal anodic oxidation dissolution. Under the high solar radiation, high salinity and high humidity corrosive environment, the metals would be corroded severely. Therefore, for development of a new metal corrosion protection technology, except need to consider the traditional corrosion-induced factors, how to suppress the influence of the light radiation in the metal corrosion process is also particularly important. The PEC cathodic protection technology is a potential method to solve this problem. If a n-type semiconductor thin film covering on the surface of metal, the solar light, especially the UV light can be absorbed by it, and then transfer to photogenerated electrons and holes. On one hand, these photogenerated electrons will shift to metal, and

cathodic protect it. On the other hand, after the UV light is absorbed competitively by the surface semiconductor thin film, the metal can be isolated from UV irradiation, to avoid corrosion accelerating. Secondly, there are two obvious differences between the PEC cathodic protection technology and the traditional PEC water splitting cells. The one is that the former does not require to pursue the ultimate photon to electric conversion efficiency, as long as the PEC thin film produces a sufficient number of photoelectrons to polarize the potential of protected metal to a cathodic protection area. Usually, the metal can be completely protected if the cathodic polarization potential higher than −300 mV (More negative polarization potential means higher performance of the metal cathodic protection. However the negative polarization potential applied on the protected metal should be less than the hydrogen evolution potential of the metal, to avoid the hydrogen embrittlement occurring on the metal). Normally, metal corrosion is a slowly process. In this case, the depletion rate of the photogenerated electrons is not quick during its PEC cathodic protection working process; However, another difference is that the CB potential of the semiconductor used in PEC cathodic protection area required negative enough (much negative than the self-corrosion potential of the protected metal), meanwhile, the VB potential of the semiconductor should be positive enough to generate holes to oxide the water without any external bias potential, only satisfied with these three conditions at the same time, the photogenerated electrons will transfer to the metal to protect it. Therefore the select scope of semiconductors in this area is much narrower than PEC water splitting. PEC cathodic protection technology is one of the potential applications in PEC field, however, it is necessary to accelerate the research rate, pushing it into practical application in the near future.

2. TiO_2 PEC cathodic protection electrode

TiO_2 as an n-type semiconductor has been broadly investigated in water splitting [13], dye-sensitized solar cells [14], photocatalysis [15], and sensors [16] due to its special chemical and physical properties. Because the valence band potential of TiO_2 is positive enough to oxide OH^- to O_2, and the negative enough CB potential, it can provide cathodic protection for some metals. When the metal is in contact with illuminated TiO_2 or coated with TiO_2 thin films, photogenerated electrons are injected from the semiconductor to the metal via the CB; As a result, the potential of the metal can be polarized to a more negative direction, so that the metal enters the thermodynamically stable region to achieve cathodic protection. Yuan and Tsujikawa [17] firstly reported that the potential of a TiO_2-coated copper substrate drastically shifted toward the negative direction under illumination in 1995. Based on this discovery, in the past two decades, the applications of TiO_2 for cathodic protection of metals have aroused widespread interest in scientific research workers. In this section, the research work based on TiO_2 will be summarized.

2.1. Testing methods of the PEC cathodic protection for metals

The photoelectrochemical test device is shown in Fig. 2-1. There are two types of tested methods. As shown in the Fig. 2-1(A), the photoanode and the protected steel electrode are connected to the workstation. The photoanode is immersed in the photo-anode cell while the protected steel electrode is placed in the corrosion cell; the two cells are connected by a salt bridge. In the photoanode tank, NaCl solution can be chosen to simulate the marine corrosive environment, or the sacrificial solution of Na_2S and NaOH (as the hole-trapping agent, S^{2-} can improve the separation efficiency of photogenerated carriers and improve the cathodic protection performance of photoelectrode), the light is shone on the surface of the photoanode through the quartz window. In addition, we can see that different films were directly coated on steel electrodes from Fig. 2-1(B). No matter what kind of tested method is, the photogenerated electrons would always transfer to the surface of the protected steel electrode, and the surface potential of the steel electrode is thereby reduced and tested by a potentiostat.

2.2. Pure TiO_2 PEC cathodic protection electrode

2.2.1. Preparation methods

At present, there are many methods to prepare TiO_2 coatings, including sol–gel, liquid phase deposition, spray

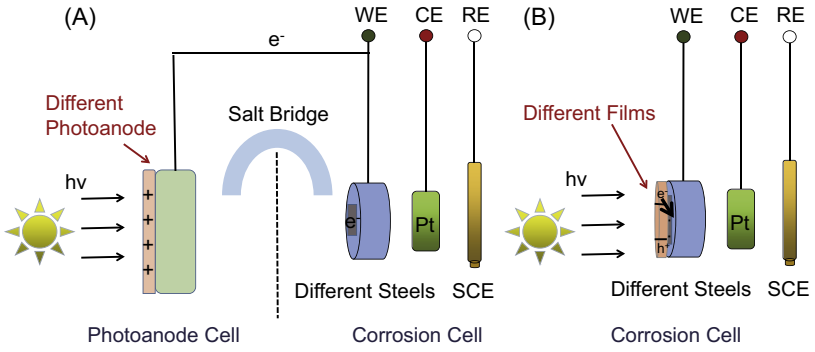

Fig. 2-1. Two types of the tested methods for PEC cathodic protection: (A) the steel coupled with different photoanodes and (B) different films were directly coated on steel electrodes.

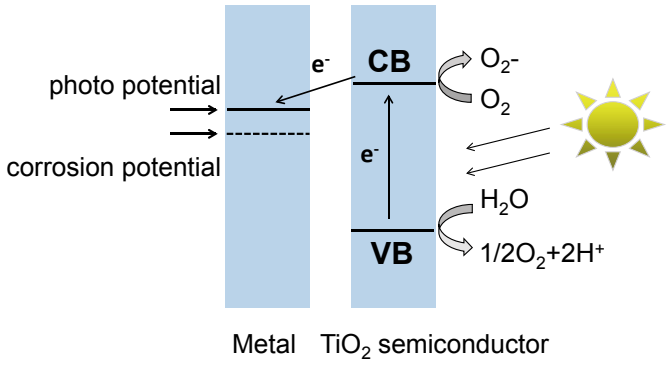

Fig. 2-2. Mechanism of the photoelectrochemical anticorrosion effect of TiO_2 for metals.

pyrolysis, anodic oxidation and hydrothermal method etc. According to the different types of contacting with metal electrodes, these techniques can be divided into PEC overlayer protection method (Preparation of TiO_2 thin film on the surface of protected metal directly) and PEC photoanode protection method (Preparation of TiO_2 thin film photoanode and ohmic contact it with metal electrode). Different preparation methods would have a great impact on the properties of TiO_2 coatings, and provide different PEC cathodic protection performance for metals. Next, we will give a brief summarize on these methods.

Sol–gel method is an economic and scalable one to fabricate TiO_2 thin film on other substrates. Yuan et al. employed this method to fabricate a TiO_2 coating on copper substrate [17]. First, the prepared TiO_2 sol by hydrolyzing Ti tetraisopropoxide in ethanol, H_2O and HCl mixture, and then the sol was coated by dipping the substrate in the sol solution and pulling it up at a constant speed. Finally, the sample was subjected to heat-treatment under the atmosphere of nitrogen. Amorphous TiO_2 gel was found to be crystallized above 400 °C which gave rise to a great enhancement of the photocurrent of the TiO_2 coating. The dramatic change in the PEC cathodic protection potential of TiO_2-coated Cu would be explained by the change of Schottky barrier at the TiO_2/Cu interface in terms of the Fermi level pinning at the Ti^{3+} defect level. Except sol–gel method, spray pyrolysis technique was also widely considered as a quick method to prepare TiO_2 thin film on other substrates. Ohko et al. [5] investigated the photoelectrochemical behavior of type 304 stainless steel (304 SS) with TiO_2 thin film coatings, fabricated by a spray pyrolysis technique. As shown in Fig. 2-2, the prepared TiO_2 coating would produce photoelectrons which are transferred directly to the metal substrate to provide a cathodic protection of the 304 SS under UV irradiation.

In order to develop more simple TiO_2-coated techniques, the liquid phase deposition (LPD) technique [18,19] was used to prepare TiO_2 films on 304 SS at a relatively low temperature (80 °C), the SEM of the TiO_2 films was shown in Fig. 2-3. It can be observed that the LPD-derived film mainly constituted of rod-like crystals with a dense and crack-free morphology. Afterwards, they further investigated the effects of the liquid-phase-deposition parameters on the performance of the TiO_2 thin films. The results showed that the LPD parameters had a significant influence on the photogenerated cathodic protection properties of the LPD-derived TiO_2 films. It was observed that the most effective photogenerated cathodic protection for 304 SS could be achieved when the TiO_2 films were prepared from the solutions containing 0.03 M $(NH_4)_2TiF_6$ and 0.09 M H_3BO_3 with the pH value of 2.9 at 80 °C for 3 h, the coupled electrodes between the TiO_2 film and 304 SS would shift to approximately −600 mV under the white light illumination. However, the disadvantage of this method was that the acidic solution would induce the corrosion of some metals in the process of TiO_2 thin films depositing. Thus the application range of the LPD method is limited (Fig. 2-4).

Because some metals are not stable in the acid deposition solution or annealing process, it is difficult to fabricate some interesting semiconductor thin films with high PEC performance on the surface of metals. Thus, to solve this problem, photoanode protection method is developed. Park et al. explored a TiO_2-based photoelectrochemical system that TiO_2 photoanode was connected galvanically with the steel electrode [6]. Under UV illumination, the TiO_2 electrode in a hole scavenging medium supplied photogenerated electrons to an electrically connected steel electrode with the generation of photocurrent and the coupled potential shifted to much more negative values. In this galvanic pair, the steel and the TiO_2 electrode acted as a cathode and a photoanode, respectively,

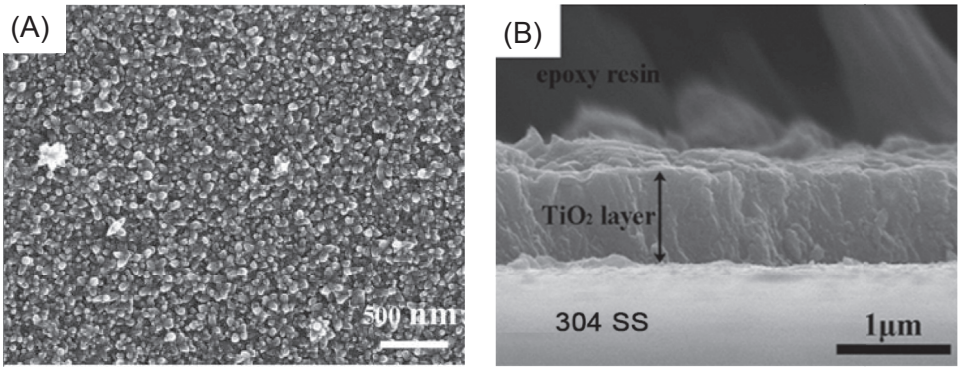

Fig. 2-3. Surface morphology of the LPD-derived film on 304 SS: a dense and crack-free morphology shown in low-magnification image (A); The cross section morphology of 304 SS substrate coated with TiO_2 thin film by three repeated LPD processes (B).

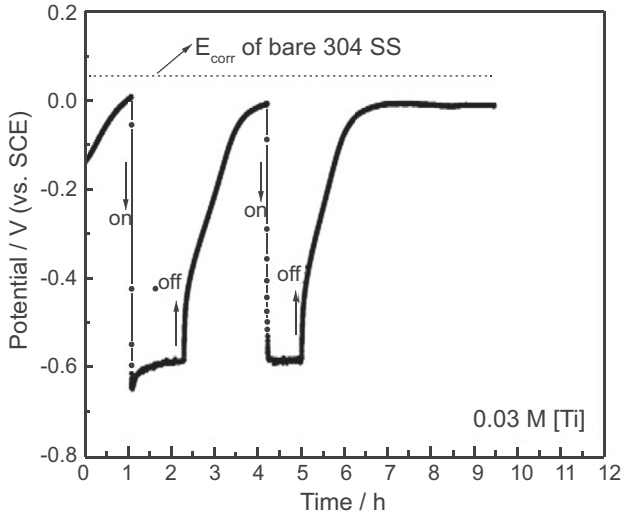

Fig. 2-4. The time evolution for the OCP of LPD-TiO_2 photoanodes prepared at the optimal $(NH_4)_2TiF_6$ concentration both under illumination and in the dark.

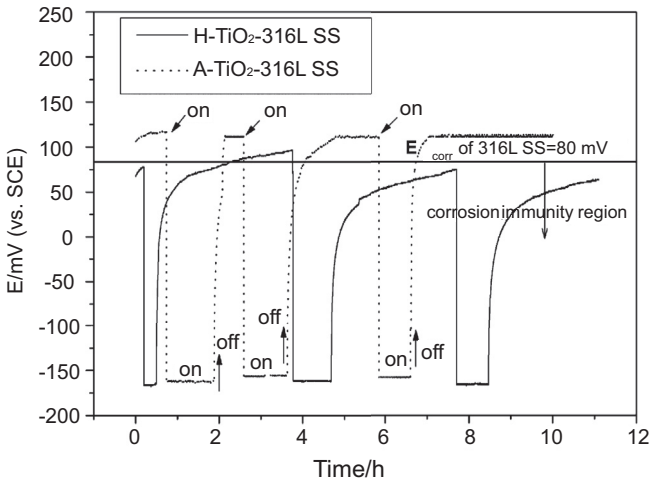

Fig. 2-6. Time evolution of the OCP of H-TiO_2-316L SS and A-TiO_2-316L SS electrodes under white light illumination and in dark condition (H-TiO_2-316L SS and A-TiO_2-316L SS represent the 316L SS coupled with the TiO_2 film prepared by hydrothermal and electrochemical anodization method, respectively).

which was essentially a variation of cathodic protection (as shown in Fig. 2-5). It was observed that the surface of steel electrode was not corroded under the UV light, but in the absence of illumination, its surface was quickly corroded, indicating that the PEC cathodic protection was real efficiency for metal anticorrosion.

For developing more efficient TiO_2 photoanode on PEC cathodic protection metals, the TiO_2 nanotube arrays (NTAs) on the surface of Ti foil prepared by the anodization method was researched [20]. The experimental results indicated that the photoelectrochemical performance of the nanoporous-structured TiO_2-NTAs was markedly influenced by the novel porous nanotubular architecture and special electrons transfer path. So the annealed nanoporous-structured TiO_2-NTAs can be deployed as one of the most promising alternative materials for the photogenerated cathodic protection of metals. Except TiO_2 NTA, Yun et al. [21] prepared a net-like structured TiO_2 film on Ti by low temperature hydrothermal method, which was mainly carried out in 10 M NaOH solution by hydrothermal etching reaction. Based on the results of the photoelectrochemical measurements, the anticorrosive behavior of the net-like structured TiO_2 film was almost equivalent to the TiO_2 nanotube arrays prepared by the anodization method, as shown in Fig. 2-6. Therefore, the hydrothermal etching method can be deployed as a feasible alternative for producing highly efficient TiO_2 films to protect metals under irradiation as well.

2.2.2. Regulation of TiO_2 films microstructure

TiO_2 photoanode with special nanostructure can improve the photoelectrochemical cathodic protection performance for metals, due to enlarging the photons capture capacity, reaction active sites and improving the charge transfer route. Therefore,

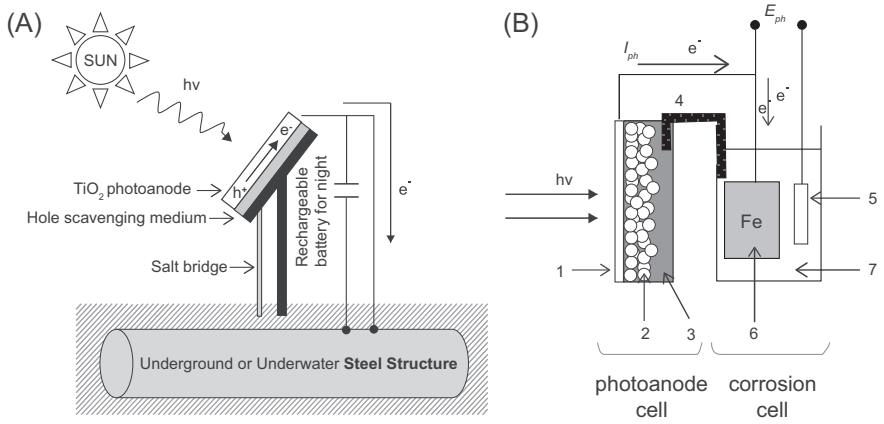

Fig. 2-5. (A) Schematic diagram of the proposed photocathodic metal protection system using a TiO_2 photoanode and solar light. (B) Experimental setup of the photoelectrochemical cell for steel corrosion prevention. The major components are (1) ITO glass, (2) TiO_2 film, (3) hole-scavenging medium containing formate (in aqueous solution or agar gel) or pure water, (4) salt bridge, (5) SCE, (6) steel electrode, and (7) electrolyte solution.

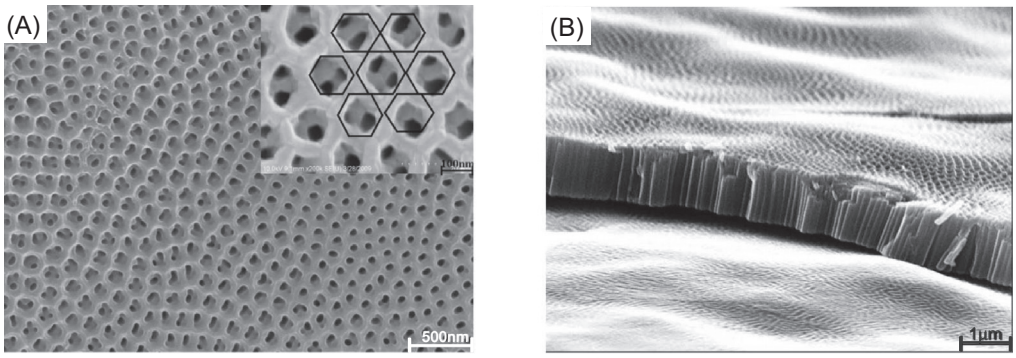

Fig. 2-7. Typical SEM images of the top and cross-sectional views for the TiO_2: (A) top view of TNs anodized in EG solution containing NH_4F (0.3 wt%) and H_2O (2.0 wt%) under 50 V; (B) cross-sectional view of (A).

it is of great significance to optimize the performance of TiO_2 photoanode by controlling its nanostructure.

Anodization or chemical etching has been identified available methods to fabricate TiO_2 thin film on Ti substrate directly. Li et al. prepared TiO_2 nanotube arrays on the surface of Ti foil by the anodization method [20]. As shown in Fig. 2-7, in the oxide layer, the nanotubes are packed closely to each other and are covered by a layer of nanoporous film at the top. It is demonstrated that the unique architecture of perfect alignment of TiO_2 NTAs is able to increase the specific surface area, and promote the separation of the photogenerated electrons and holes, which is obviously better than that of the traditional dense thin films.

Li et al. [22] employed anodization method to prepare TiO_2 films at high voltages. TiO_2 film formed at 120 V could serve as photoanode and supply a protective photocurrent about 8 $\mu A/cm^2$ to carbon steel in 3% NaCl solutions. From the fitted results of EIS spectra for different TiO_2 films, the film resistances were only about several 10 $\Omega\ cm^{-2}$ under UV illumination conditions, therefore photogenerated electrons were gradually accumulated in the TiO_2 films, resulting in negative shifts. But TiO_2 films could accelerate the corrosion of carbon steel in the dark, and the protective coupling current was relatively small, so further effort was required for a complete photocathodic protection of carbon steel by anodic TiO_2 films (Fig. 2-8).

A net-like structured TiO_2 film was obtained with a low-temperature hydrothermal process, also offered a distinctly photogenerated cathode protection for 316L SS under the white light illumination [21]. Some special nanostructure TiO_2 thin film can also be prepared by sol–gel method. Lei et al. [23] prepared a ordered mesoporous TiO_2 thin films through the sol–gel and evaporation-induced self-assembly method, and served them as photoanodes for 304 SS PEC cathodic protection. The results showed that mesoporous TiO_2 films calcined at 500 °C exhibited more negative photoinduced potential and larger photocurrent than that calcined at 350 °C. This phenomenon was attributed to obtaining higher crystallinity for the ordered mesoporous TiO_2 films upon calcination at 500 °C, which could allow for the more effective transfer of photogenerated electrons in the TiO_2 layers. Besides, the ordered mesoporous microstructure in the TiO_2 films would absorb more amounts of HCOO• group which could provide a faster and more direct pathway for electrons transfer under illumination (Fig. 2-9).

A combined sol–gel and hydrothermal method was developed to prepare a 3D titanate nanowire network film on titanium substrates, and gain an especial PEC cathodic protection effect for 403 SS [24]. The electrode potential of 403 SS in a 0.5 M NaCl solution decreased by 560 mV when it was coupled to the as-prepared 3D titanate nanowire film under illumination. Especially, when the light source cut off, the photoinduced potential of the steel turned back by only 50–145 mV, and kept it lower than the corrosion potential for over 10 h, which indicated that the 3D titanate nanowire network film could produce a striking photocathodic protection effect for 403 SS under illumination and continual protection at dark conditions. There were two main reasons: firstly, the striking effect of the titanate film might result from its particular structure which possessed a large surface area to enhance the absorption of light. Secondly, the structure with hollow nanowires facilitates the orientated transference of

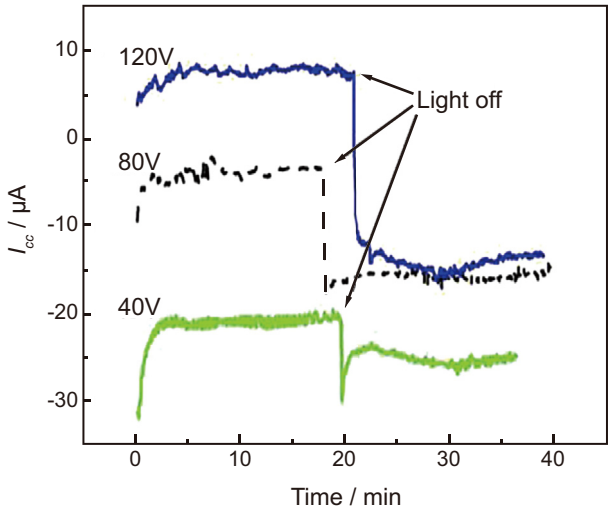

Fig. 2-8. Variations of coupling currents with time for the TiO_2 film-carbon steel galvanic couples under conditions of light on and off.

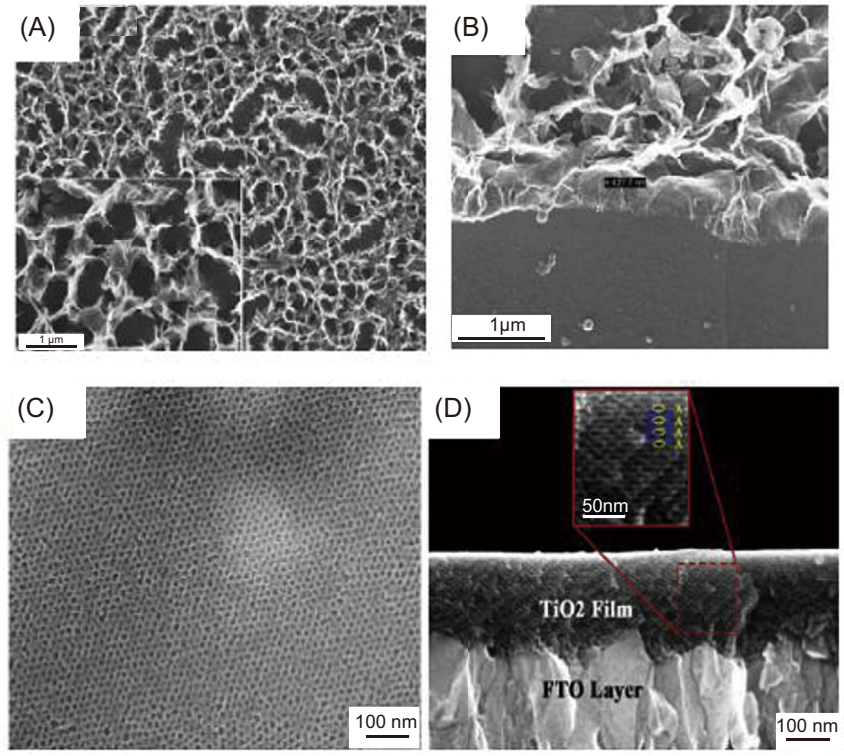

Fig. 2-9. (A) the top view of the TiO_2 films obtained by 2 h of hydrothermal reaction at 140 °C; The inset shows a high magnification image of the film; (D) the cross-section of (B); the surface and cross sectional morphologies of the mesoporous TiO_2 films calcined at 350 °C (C) and (D).

electrons, which might be effective to reduce the recombination rate of photogenerated electrons and holespairs. Based on the above characteristics, the 3D titanate nanowire network film can provide an effective PEC cathodic protection performance for metals.

Shen et al. [25] developed a combined sol–gel and hydrothermal post-treatments method to prepare a uniform TiO_2 nanoparticle coating on steels. It indicated that the TiO_2 nanoparticle coating with about 460 nm thickness exhibit an excellent corrosion resistance in the 0.5 mol/L NaCl solution. It is evident that corrosion potential positively shifts, i_{corr} decreases by 3 orders of magnitude, and corrosion resistance R_t increases more than 100 times after applying a TiO_2 nanoparticle coating on 316L stainless steel comparing with bare steel in the same environment. Under UV irradiation, the photogenerated electrons result in a potential shift of metal substrate to the corrosion immunity region. Furthermore, the TiO_2 nanoparticle coatings on steels exhibit an excellent corrosion resistance due to a ceramic protective barrier on metal surface in dark (Fig. 2-10).

2.3. Doped TiO_2 PEC cathodic protection electrode

2.3.1. Metal doping

TiO_2 is a wide band gap semiconductor material ($E_g = 3.2$ eV), and only responds to ultraviolet that accounted for only 3–4% of solar light, thus affecting the photoelectrochemical cathodic protection of metals. Considering utilizing the solar energy more effectively, intensive efforts have been carried out to shift the response range of TiO_2 to

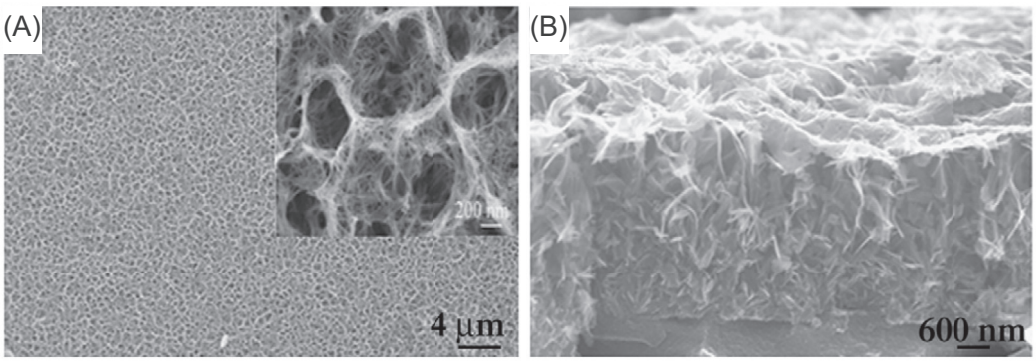

Fig. 2-10. (A) Surface and (B) cross-sectional SEM images of a titanate nanowire film prepared by a combined sol–gel and hydrothermal method.

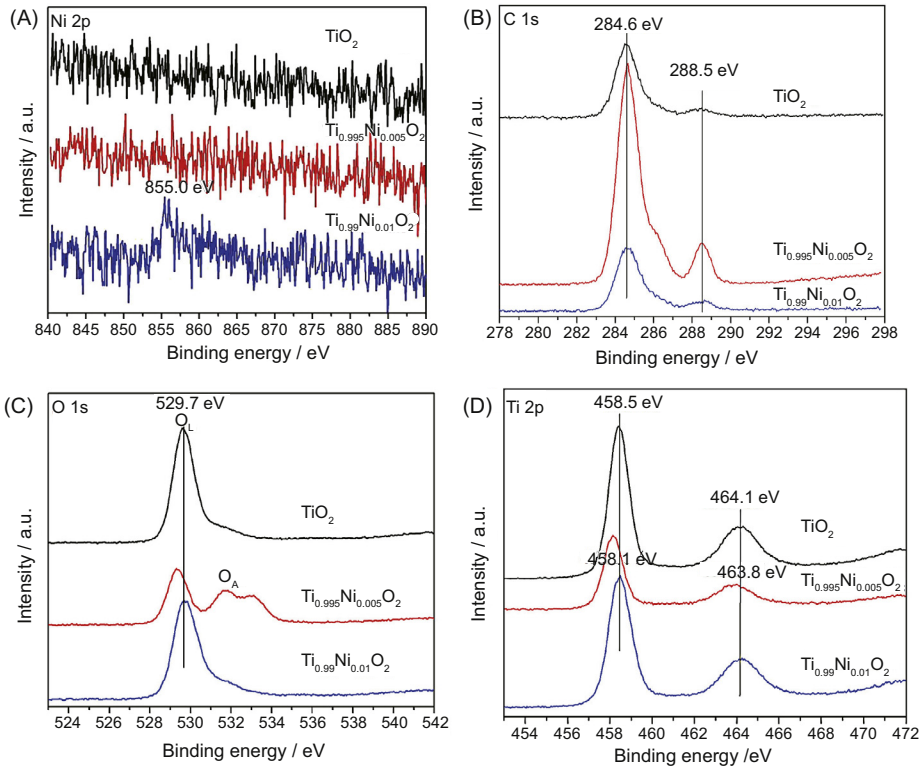

Fig. 2-11. Ni 2p (A), C 1s (B), O 1s (C) and Ti 2p (D) XPS spectra of $Ti_{0.995}Ni_{0.005}O_2$ and $Ti_{0.99}Ni_{0.01}O_2$ (O_A: adsorbed oxygen; O_L: lattice oxygen).

visible light. It is reported that doping by metal or nonmetal element is a feasible method to achieve this purpose.

Ni-doped TiO_2 photoanode, which was fabricated via sol−gel method [26], possessed the excellent photoelectrochemical anticorrosion property for 304 SS under visible light illumination. It was found by UV−vis diffuse reflection that the absorption band-edges of Ni-doped TiO_2 was red-shift to visible light region (420−520 nm) after doping with Ni. This result was mainly attributed to that Ni substituted the Ti^{4+} lattice sites, as shown in Fig. 2-11, resulting in the oxygen vacancy formation. The oxygen vacancy promotes the transfer of photoinduced electrons, to increase the photo-to-current conversion efficiency of TiO_2 under visible light further.

Except that red shifts the light response range of the TiO_2 thin film, doping some specific elements can also provide additional functions for it during PEC cathodic protection process. Li et al. [27] prepared a series of chromium-doped TiO_2 coatings for corrosion protection of 316L stainless steel substrates. The corrosion protection performances of the coatings in the presence and absence of simulated sunlight illumination were evaluated through electrochemical measurements. It was found that the photoelectrochemical cathodic protection performance of chromium-doped TiO_2 coating was significantly improved. Among them, the PEC cathodic protection potential of 1% Cr−TiO_2 coating shifted the most negative value under illumination, which was 230 mV lower than the corrosion potential of 316L stainless steel. Additionally, under the dark condition, the chromium-doped TiO_2 coatings can provide not only mechanical covering of the metal surface but also active corrosion protection due to the self-healing property of chromium ions. Furthermore, they had successfully prepared the smooth and compact cerium ion-doped nano-TiO_2 coating on the 316L stainless steel by the sol−gel and dip-coating techniques [28]. The cerium ion-doped nano-TiO_2 overlayer can also improve the photo-to-current-conversion efficiency of TiO_2, and act as a better anticorrosive barrier under the dark condition (Fig. 2-12).

Liu et al. [29] fabricated Fe-doped TiO_2 thin films by LPD method, using Fe(III) nitrate as both Fe element source and

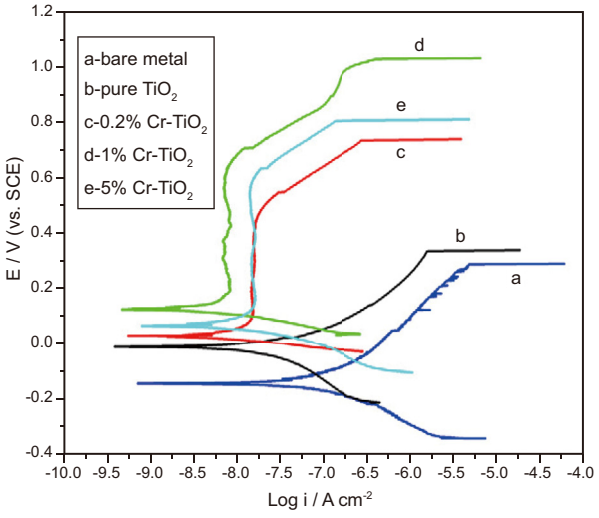

Fig. 2-12. Potentiodynamic polarization behaviors of bare metal and the Cr−TiO_2 coatings with the mole ratio of Cr/Ti = 0%, 0.2%, 1%, and 5% on 316L stainless steel.

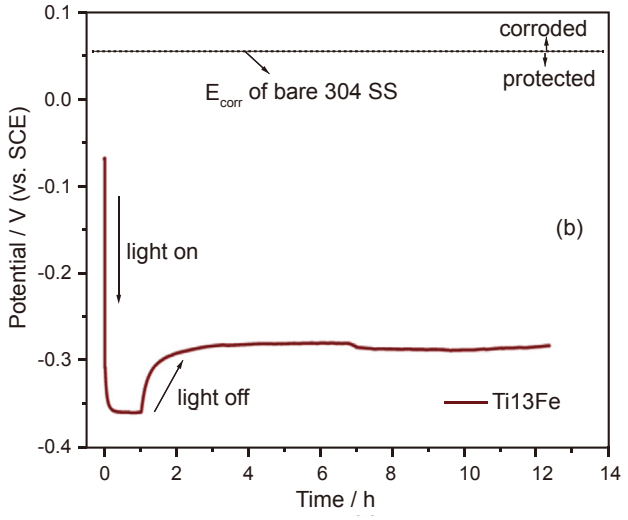

Fig. 2-13. Charge and self-discharge properties of Ti13Fe electrode.

fluoride scavenger instead of commonly-used boric acid (H_3BO_3). Compared with plain TiO_2 films, the photoelectrochemical properties of the Ti13Fe (Fe/Ti = 3 M ratio) thin film prepared in precursor bath containing 0.02 M TiF_4 + 0.06 M $Fe(NO_3)_3$ was significantly enhanced under white-light illumination. Furthermore, keeping to be irradiated for 1 h, the potential of 304 SS could maintain in a narrow range of −280 to −250 mV lower than its corrosion potential exceed 12 h even after the light was cut off (Fig. 2-13).

2.3.2. Nonmetal doping

Nonmetal element doping method has also been widely accepted as an effective method to shorten the bandgap of TiO_2 via induce a doping energy level above its valence band. Li et al. [30] prepared a highly ordered n-doped TiO_2 nanotube layers on Ti substrate by a self-organized electrochemical anodization and wet doping process in nitrogen sources contained fluorinated electrolyte. It is shown that the nitrogen ions substitute oxygen atoms in the TiO_2 lattice and thus the corresponding N 2p states are located above the valence band edge, providing a significant response in the visible light region. It is noted in Fig. 2-14, that the annealed n-doped TiO_2 nanotube sample curves (a, b, c) has a significantly enhanced of the photocurrent response in the visible range of the spectrum, but for the pure TiO_2 nanotube films (curve d), no photocurrent can be observed in visible light region at the same experimental conditions.

Similarly N-doped nanoflower-like TiO_2 film, which prepared by a low-temperature hydrothermal reaction [31], could provide a significant visible light response and enhance the photocurrent dramatically in both the UV and the visible light range. As shown in Fig. 2-15(A), the N-doped samples showed a much stronger photo absorption capacity from 470 to 650 nm, compared with the pure TiO_2 nanotube layers with predominant photo absorption at the edge of 300 nm. The absorption edge of the N-doped TiO_2 nanolayers obtained after 12 and 60 h occurred at about 650 and 570 nm, and the corresponding band gap energy could be estimated to be 1.91 and 2.17 eV, respectively, which are much smaller than that of pure TiO_2 band gap (3.2 eV). Fig. 2-15(B) gives a comparison of the electrode potential of 316L SS coupled with the N–TiO_2 film electrodes under UV (curve d, λ = 350 nm), visible light (curve c, λ = 550 nm) illumination, and in the dark. It can be found that the photoinduced potential drop is very small and unstable under UV illumination, but under the irradiation of visible light, the photo-induced potential drop is very large and relatively stable, and this potential drop can maintain for a long period after light cut off.

In addition, a N-F-codoped TiO_2 film, which prepared by liquid-phase-deposition (LPD) method [32], was also served as a photoanode for the cathodic protection of 304 SS. The experimental results indicated that the LPD-TiO_2 films showed a visible-light response in the wavelength range of 600–750 nm. With the heat treatment temperature increased, the photocurrent intensities were enhanced in both the

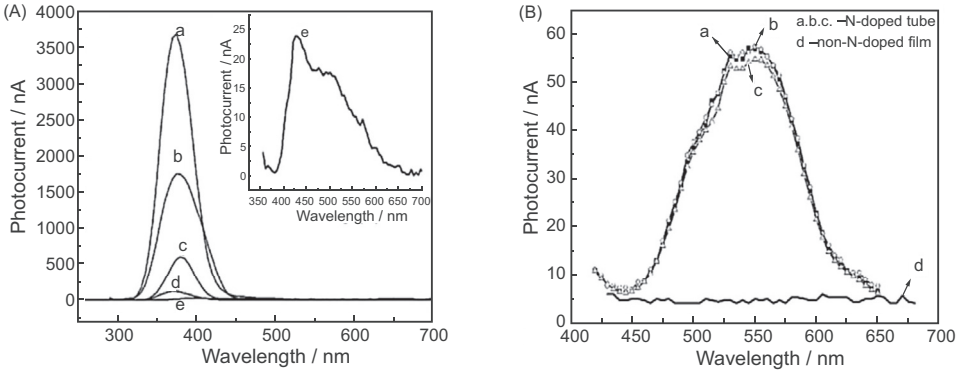

Fig. 2-14. (A) A comparison of photocurrent spectra of the pure TiO_2 nanotubes film and the nanoparticles film, recorded under bias of 300 mV: TiO_2 nanotube layers anodized in 0.2 M Na_2SO_4 + 0.5 wt % NaF under 20 V for 4 h curve (a); TiO_2 nanotube layers anodized in 1 M H_2SO_4 + 0.15 wt % HF under 20 V for 2 h curve (b); TiO_2 nanoparticle films prepared by the regular sol–gel method curve (c); blank titanium substrates curve (d); n-doped TiO_2 nanoparticle film curve (e). (B) A comparison of photocurrent spectra of the n-doped curves (a, b, c) and no-n-doped curve (d) TiO_2 nanotube films recorded under the different bias voltages: (a) 1 V, (b) 3 V, (c) 300 mV, (d) 3 V.

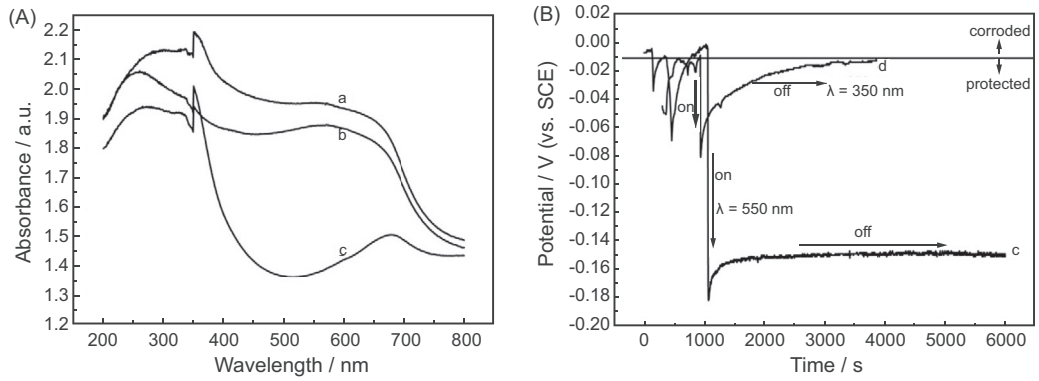

Fig. 2-15. (A) A comparison of UV−vis absorption spectra of the flower-like N-doped TiO_2 films and the non doped TiO_2 nanotube arrays annealed at 450 °C: N−TiO_2 films after 60 h of hydrothermal reaction (curve a); N−TiO_2 films after 12 h of hydrothermal reaction (curve b); TiO_2 nanotube anodized in 0.2 M Na_2SO_4 + 0.5 wt% NaF + glycerol electrolyte for 5 h (curve c); (B) Time dependence of electrode potentials for 316L SS coupled with the N-doped TiO_2 nanoporous films electrodes under visible light (curve c) and UV illumination (curve d).

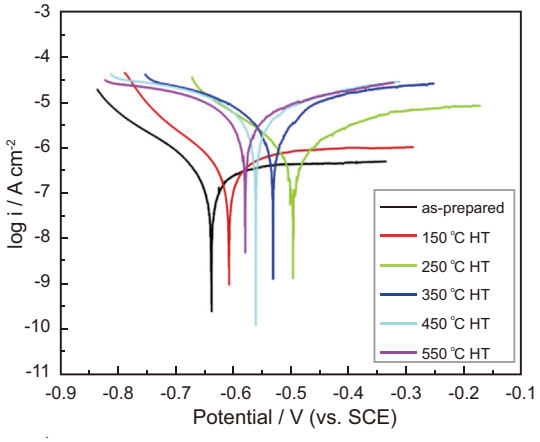

Fig. 2-16. The Tafel polarization curves of the TiO_2 films and 304 SS electrodes before coupling both in the dark and under white-light illumination.

ultraviolet UV-light and visible-light regions. However, the as-prepared pure LPD-TiO_2 films exhibited the most negative photopotential under both visible-light and white-light illumination. It is mainly contributed that the higher crystallinity of the heat-treated LPD-TiO_2 films would allow the photogenerated electrons to move faster in the space-charge layer (Fig. 2-16).

2.4. Compounded TiO_2 PEC cathodic protection photoanode

The wide band-gap of TiO_2 (3.2 eV) limits its response within the UV light region. Although doping can shorten the forbidden band-gap, the doping level is mostly indirect and the absorption efficiency of photons is relative low. At the same time, doping may introduce new recombination center to the crystal, which leads to the decrease of PEC performance. Thus, for solving this problem, researchers combined TiO_2 with other semiconductor materials to create a heterojunction field at their interface, and enlarge the light response range by the compound semiconductors.

2.4.1. Sensitized TiO_2 PEC cathodic protection photoanode

Li et al. [33] deposited CdS nanoparticles on the surface of anodic TiO_2 nanotubes (TNs) by a simple DC electrochemical deposition method in a mixed electrolyte of $CdCl_2$ and dimethylsulfoxide. Compared with pure TNs, as shown in Fig. 2-17, CdS-TNs showed a significantly enhanced

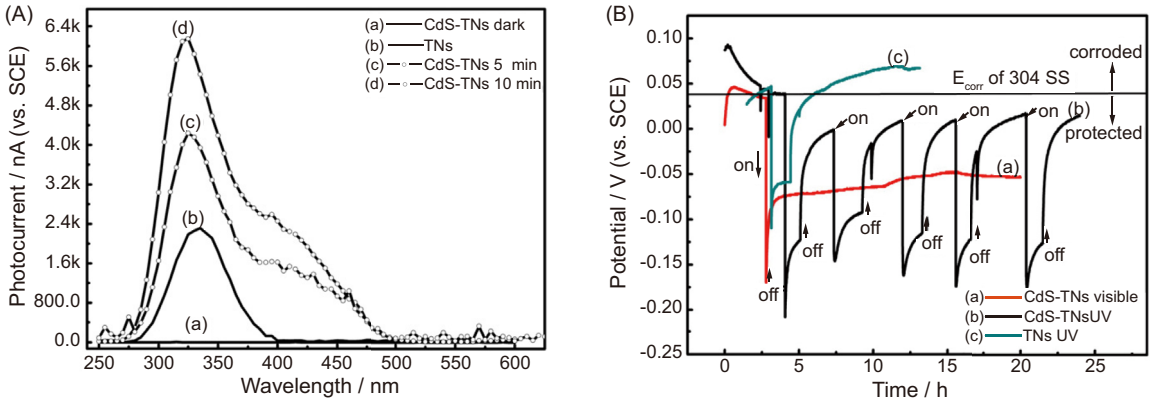

Fig. 2-17. Photocurrent spectra of the pure TNs and various CdS-TNs electrodes (A) and OCP variations for 304 SS coupled with CdS-TNs electrodes under white light (curve a) and UV illumination (curve b), TNs under UV light (λ = 360 nm) (curve c), and in dark conditions (B).

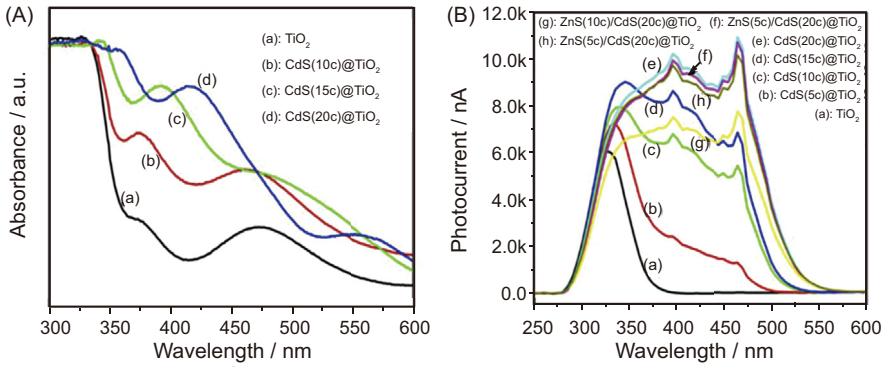

Fig. 2-18. UV–visible absorption spectra (A) and photocurrent spectra (B) of TiO_2 NTs and series of compound electrodes.

photocurrent response that extended to 480 nm. The high optical activity of the CdS-TNs compound semiconductor system is attributed to the strong absorption in the solar spectrum, the efficient electron transfer of electrons and the separation of electron–hole pairs in the regular TiO_2 nanotube structure. It was found that the potential of the 304 SS electrode coupled with the CdS-TNs electrode in the NaCl solution shifted about 246 mV and 215 mV, respectively, under UV and white light irradiation. Even after the light was cut off, the negative potential could remain for several hours. The results showed that the CdS-sensitized TiO_2 nanotube film can effectively protect the metal from the corrosion.

Lin et al. [34] deposited ZnS/CdS quantum dots (QD) of core–shell nanostructures on the surface of TiO_2 nanotubes by chemical bath deposition (CBD) in an alcoholic solution system. The experimental results showed that with the increase of CdS quantum dots amounts, the light absorption range of the compound photoanode gradually expanded to the visible light region, and the intensity of photocurrent was obviously enhanced (see Fig. 2-18). The nanostructured CdS QDs (20 cycles) coated on TiO_2 nanotube arrays showed a remarkably enhanced photoelectrochemical activity. The coating of ZnS QD shell (5 cycles) could significantly improve the stability of CdS@TiO_2 photoanode under white light irradiation. In addition, the photoanode showed better PEC activity in 0.1 M Na_2S + 0.2 M NaOH mixed solution than in 0.1 M Na_2SO_4 solution. The potential of the 403 SS electrode coupled with CdS(20c)@TiO_2 photoanode was negatively shifted under the white light irradiation. However, with the increase of the tested time, the potential of 304 SS electrode coupled with ZnS(5c)/CdS(20c)@TiO_2 photoanode could be negative shifted by 900 mV, and still maintained at a long time. It could also provide a certain extent of corrosion protection for the 304 SS electrode in the dark.

Except unstable CdS, Li et al. [35] prepared Ag and SnO_2 co-sensitized TiO_2 photoanode by photo-reduction deposition and sol–gel method, and their morphology, crystalline phase, composition and optical absorption properties were studied systematically. The results showed that the co-sensitization of Ag and SnO_2 shifts the light absorption of TiO_2 to the visible light, and the Schottky barrier between Ag and SnO_2 can be effectively prevented, the recombination of photo-generated electrons and holes, thus improve the separation efficiency of photo-generated charges. The SnO_2 coating prepared by the sol–gel method can be used as energy storage material to accept the photo-generated electrons from TiO_2, so that the co-sensitized TiO_2 photoelectrode can not only exhibit highly effective photogenerated cathodic protection performance to 304 SS, but also provide delay protection for the stainless steel in the dark, as shown in Fig. 2-19.

2.4.2. Carbon composite TiO_2 PEC cathodic protection electrode

To date, the optical absorption range of the visible light-sensitized TiO_2 composites were effectively extended, and the metal corrosion protection by the TiO_2 composite materials photoanode was also enhanced, but the charge transfer capacity of the TiO_2 photoanode was not high enough. Thus, developing some charge transfer materials and compounding them with TiO_2 photoanode is a potential method. The carbon nanotubes (CNTs) are considered to be one of the most promising materials because of their excellent electronic, thermal and mechanical properties [36]. In fact, some studies have

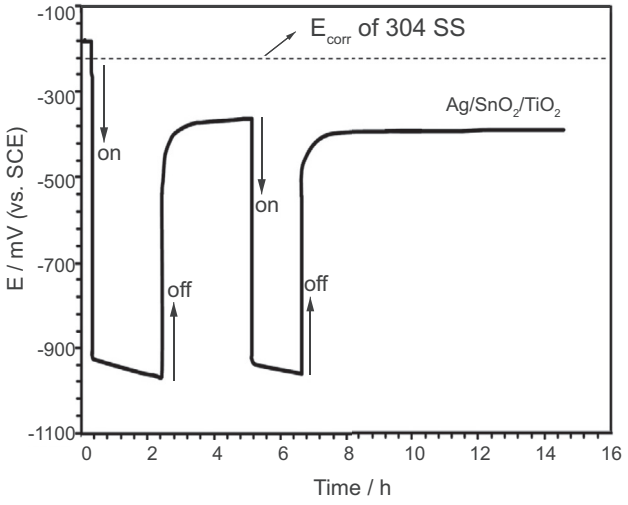

Fig. 2-19. OCP variations of a pure 304 SS electrode coupled with Ag/SnO_2/TiO_2 after the third use under intermittent illumination with visible light ($\lambda > 400$ nm).

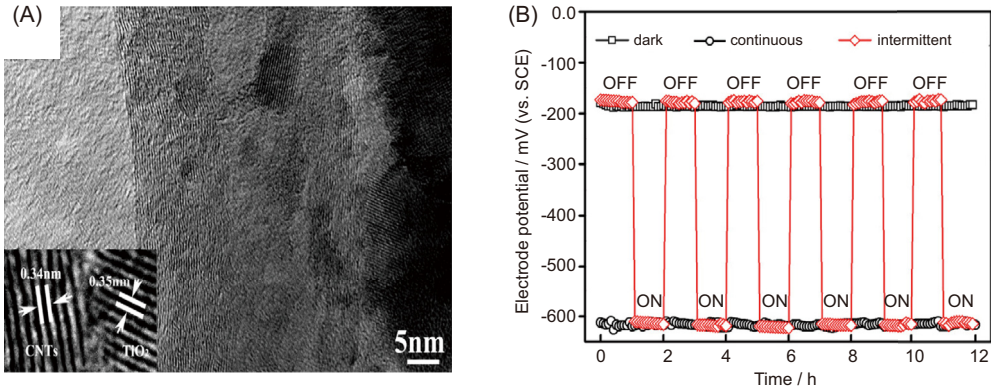

Fig. 2-20. (A): the HRTEM image of the composite film and the high-magnification HRTEM image of the interface between carbon tubes and the TiO_2 nanoparticles (left inset); (B): Potential changes of the sample (1C + 1T) under different illumination conditions of dark, continuous, and intermittent light.

demonstrated that the accepting electron and transport properties of CNTs are very favorable for the rapid transport of photogenerated carriers [37]. In general, the construction of CNTs and TiO_2 composite thin films has a dual functions. Firstly, their seamless tubular structure allows only the axial movement of electrons, which will facilitate the rapid transfer of photogenerated electrons. On the other hand, the charge collection of CNTs effectively reduces the recombination of the charge carriers, thus enhancing the PEC properties of the TiO_2 films. Liu et al. [38] successfully prepared composite films of TiO_2 and multiwall carbon nanotubes (MWCNT) on 304 stainless steel (304 SS) by sol–gel method and annealing treatment. The corresponding test results are shown in Fig. 2-20. The preparation parameters of the films were optimized by measuring the amount of MWCNTs, the thickness of the films and the PEC cathodic protection properties. Corresponding results of electrochemical tests showed that the MWCNT/TiO_2 composite films possessed better corrosion protection performance under dark or ultraviolet irradiation to 304 SS than pure TiO_2 films. The high conductivity of MWCNT in the MWCNT/TiO_2 composite film can easily transfer the photo-generated electrons to the metal substrate and restrain the recombination of the

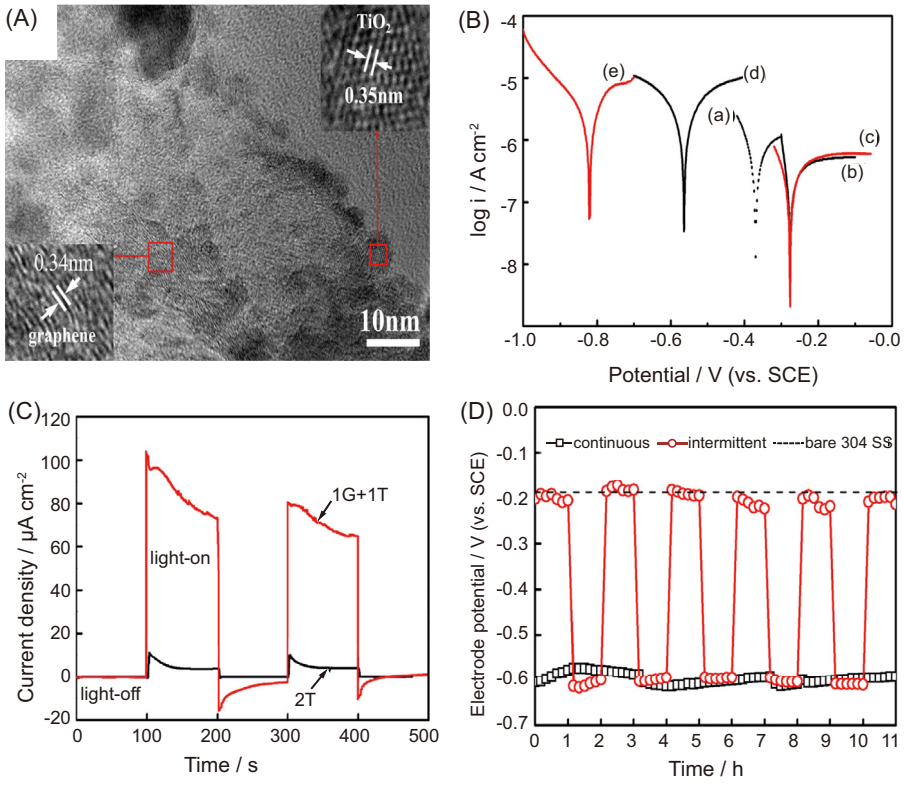

Fig. 2-21. (A): The HRTEM image of the fragments of the composite film and the high magnification HRTEM image of G (left inset) and TiO_2 particles (right inset); (B): Comparison of the polarization curves for the (1 GT + 1T) sample and the 304 SS covered by double pure TiO_2 layers (2T sample) in the presence and absence of UV illumination and for bare 304 SS in the dark; (a) bare 304 SS in the dark. (band d) the (2T) sample in the dark and under illumination; (c and e) the (1 GT + 1T) sample in the dark and under illumination; (C): Variations of coupling currents with time for the (1 GT + 1T) sample, and the (2T) sample with under UV illumination; (D): Potential changes of the (1 GT + 1T) sample under different illumination conditions of continuous and intermittent light.

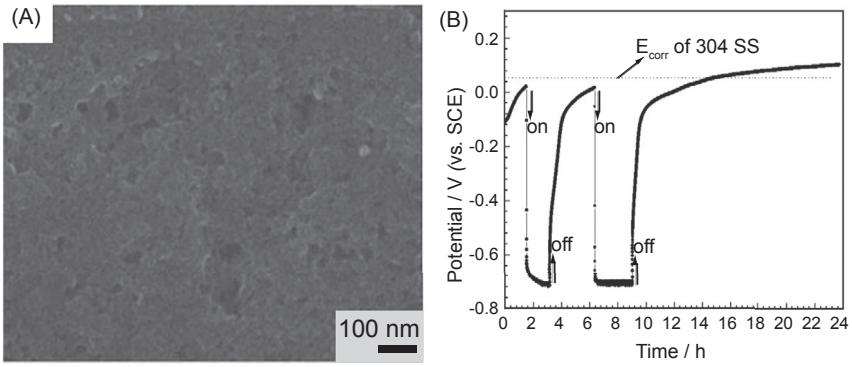

Fig. 2-22. The surface morphologies of LPD-derived sodium polyacrylate/TiO_2 hybrid films on FTO substrates prepared at the sodium polyacrylate concentrations of 0.5 g/L (A); The time evolution of the open-circuit potentials (OCP) of the sodium polyacrylate/TiO_2 films prepared at the sodium polyacrylate concentrations of 0.5 g/L.

electron–hole pairs, so the composite film exhibits three times higher photocurrent than the pure TiO_2 film but only half of the charge transfer resistance.

Liu et al. continued to study the PEC cathodic protection performance of TiO_2 and graphene (G) composite films on the 304 SS electrode by the above methods [39]. As shown in Fig. 2-21, the corrosion protection performances of composite films to 304 SS in 3.0% NaCl solution were evaluated by electrochemical tests. The PEC cathodic potential of TiO_2 thin film could be significantly improved after 0.5% graphene composite in. Under the irradiation of UV light, this composite photoanode could provide a −600 mV cathodic potential drop for 304 SS. In addition, it showed a 14 times higher photocurrent density than that of the pure TiO_2 film, because of the excellent electrical conductivity of graphene and the large contact area between it and TiO_2 particles. Therefore, the introduction of nano-carbon materials into TiO_2 film is a promising technology to improve the PEC cathodic protection to metals.

2.4.3. Polymer modified TiO_2 PEC cathodic protection electrode

In addition to the above-mentioned TiO_2 composite photoanode, the polymer/TiO_2 composite thin film prepared by the one-step method presented a excellent PEC cathodic protection performance also. Some studies had found that the addition of organic materials in the LPD process can improve the electrochemical and PEC properties of TiO_2. However, there were few studies on the PEC cathodic protection of organic-TiO_2 hybrid films by LPD method. Lei et al. [40] successfully prepared sodium polyacrylate/TiO_2 composite film by the liquid deposition method for cathodic protection. The results showed that (see Fig. 2-22) the composite film has a porous microstructure compared with the pure TiO_2 film, and showed

Table 1
the date summary for PEC cathodic protection performance of TiO_2.

Photoanode	Method	Photosource	OCP (mV)	Metal	Literature
Pure TiO_2	Sol–gel	UV light	600	Cu	[17]
Pure TiO_2	Spray pyrolysis	UV light	250	304 SS	[5]
Pure TiO_2	LPD	White light	655	304 SS	[19]
Pure TiO_2	Anodization	White light	354	304 SS	[20]
Pure TiO_2	Hydrothermal	White light	262	316L SS	[21]
Pure TiO_2	Sol–gel	White light	525	304 SS	[22]
Pure TiO_2	Sol–gel	UV light	439	316L SS	[23]
Pure TiO_2	Sol–gel, hydrothermal	White light	560	403 SS	[24]
Ni–TiO_2	Sol–gel	Visible light	300	304 SS	[26]
Cr–TiO_2	Sol–gel	Simulated sunlight	230	316L SS	[27]
Fe–TiO_2	LPD	White light	405	304 SS	[29]
N–TiO_2	Anodization	Visible light	400	316L SS	[30]
N–TiO_2	Hydrothermal	UV light	470	316L SS	[31]
N–F–TiO_2	LPD	Visible light	515	304 SS	[32]
CdS/TiO_2	Anodization	UV light	246	304 SS	[33]
	Electrochemical deposition	White light	215	304 SS	
ZnS/CdS@TiO_2	Anodization	White light	900	403 SS	[34]
	Electrochemical deposition				
Ag/SnO_2/TiO_2	Photo-reduction deposition, sol–gel	Visible light	550	304 SS	[35]
MWCNT/TiO_2	Sol–gel	UV light	400	304 SS	[38]
GR/TiO_2	Sol–gel	UV light	400	304 SS	[39]
Sodiumpolyacrylate/TiO_2	LPD	White light	710	304 SS	[40]

stronger photocurrent in the UV and visible light illumination as well. The best one polyacrylate/TiO_2 composite films can provide a near −710 mV cathodic potential drop for the 304 SS. Therefore, the preparation of organic/TiO_2 composite film by liquid deposition method is a new strategy for metal PEC cathodic protection thin film fabrication.

Table 1 summarizes the PEC cathodic protection properties of TiO_2 photoanodes. As this results, we can find that TiO_2 photoanodes prepared by LPD method show much higher cathodic protection OCP drop than these TiO_2 photoanodes prepared by other methods, meaning that LPD is an important method to fabricate TiO_2 photoanode with high quality. For the modified TiO_2 photoanodes, ZnS/CdS@TiO_2 and Ag/SnO_2/TiO_2 present higher PEC cathodic protection performance than the doped TiO_2 photoanode under visible light illumination. However, the ZnS/CdS@TiO_2 and Ag/SnO_2/TiO_2 photoanode show a much lower stability than doped TiO_2 photoanode during working. So the doped TiO_2, especially N−F co-doped TiO_2 photoanode possesses significant research and application potential. Furthermore, from this table we can find that the protected metals by TiO_2 based photoanodes are some difficult corrosion metals with positive enough self-corrosion potentials. This phenomenon is determined by the conduction band potential of TiO_2, which means it is more negative than the self-corrosion potentials of these protected metals (such as Cu and some stainless steels). However, for some widely used metals with more negative self-corrosion potential, such as carbon steels and weathering steels, TiO_2 based photoanodes are not suitable, because the photogenerated electrons by TiO_2 based photoanode can't overcome the energy barrier during the process of transfer to metals. Thus, some n-type semiconductors with more negative CB potential such as titanate semiconductors should be developed to protect them.

3. $SrTiO_3$ PEC cathodic protection electrode

$SrTiO_3$ is one of the semiconductor materials with a perovskite structure (ABO_3), whose bandgap width is about 3.2 eV. $SrTiO_3$ possesses many excellent properties, such as superconductivity, magnetic ferroelectric, large dielectric constant, photoluminescence, excellent chemical stability, that can be applied to the capacitor, vessel materials, photocatalytic materials, high-temperature superconducting carrier and many other areas. $SrTiO_3$ was familiar to people as a kind of efficient photocatalyst at the first time [41–44]. And $SrTiO_3$ shows the better performance than TiO_2 in many photochemical areas, such as photocatalytic degradation of organic compounds [45], PEC hydrogen production [46]. This can be owing to the difference of energy band potential between $SrTiO_3$ and TiO_2.

As is shown in Fig. 3–1, $SrTiO_3$ has a more negative CB potential, which can greatly promote the cathodic process in the PEC reaction, so the performance of photocatalytic degradation of pollutants and PEC hydrogen production is better than that of TiO_2. What's more, the more negative CB

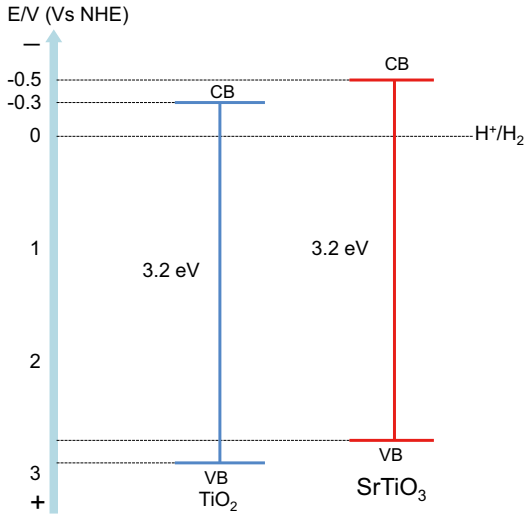

Fig. 3-1. The energy band potential distribution of TiO_2 and $SrTiO_3$.

potential is very favorable for the PEC cathodic protection. To date, in the aspect of PEC cathodic protection, more researches are focused on the cathodic protection of 304 stainless steel. Carbon steel is a kind of cheaper and more widely used steel. However, from the view of thermodynamics, it is very difficult for TiO_2 to produce a cathodic protection effect on the carbon steel, due to the more negative self-corrosion potential of carbon steel compared with 304 stainless steel. The CB edge of $SrTiO_3$ is −200 mV more negative than that of TiO_2 [47], as a result the photogenerated electrons with strong reduction capacity can easily overcome the energy barrier between the semiconductor and the metal, and smoothly transfer to the metal substrate to form a cathodic protection. Therefore, $SrTiO_3$ is a kind of feasible material used for the PEC cathodic protection of carbon steel.

3.1. $SrTiO_3$ PEC cathodic protection electrode

3.1.1. Preparation technology of $SrTiO_3$ PEC cathodic protection thin film

There are abundant preparation technologies of $SrTiO_3$, including high temperature solid-state reaction method [48], hydrothermal method [49], sol–gel method [50], chemical co-precipitation method [51]. $SrTiO_3$ powders can be obtained by using these methods. Therefore, in order to meet the requirements of the PEC cathodic protection, the $SrTiO_3$ powder should be putted on FTO or other conductive substrate to form a thin film by the method of dot-coating or electrophoresis. Dot-coating method has been widely used in the preparation of the film photoelectrode. Bu [50] prepared $SrTiO_3$ powder using sol–gel method, and then $SrTiO_3$ homogenate was evenly coated on the conductive glass by dot-coating to form a $SrTiO_3$ thin film photoanode. Electrophoresis method has not been widely used in the preparation of $SrTiO_3$ thin film. But the surface of the electrode prepared by electrophoresis method is more uniform, so the electrophoretic method can be applied to

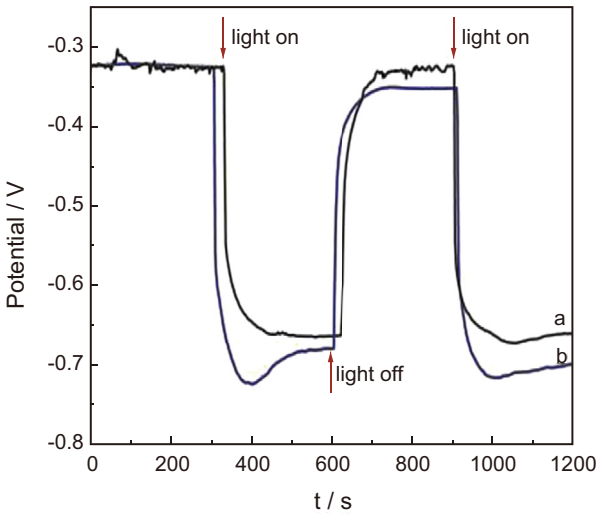

Fig. 3-2. Open circuit potentials measured on 304 stainless steel samples coupled with photoelectrodes coated with different $SrTiO_3$ powders prepared in the absence (a) and presence (b) of CTAB with and without simulated solar light illumination.

the preparation of $SrTiO_3$ thin films. Except $SrTiO_3$ thin film prepared by powder, some researchers employed TiO_2 nanotubes array as the template to prepare $SrTiO_3$ photoanode, thus $SrTiO_3$ can be prepared on the titanium sheet directly. Jiao [52] prepared TiO_2 nanotubes by anodic oxidation method on titanium sheet, then the TiO_2 nanotubes were placed in $Sr(OH)_2$ aqueous solution and after hydrothermal reaction, some TiO_2 nanotubes could be transformed into $SrTiO_3$. So the prepared $SrTiO_3$ thin film can be directly used as photoanode for PEC cathodic protection performance assessment.

3.1.2. PEC cathodic protection performance of $SrTiO_3$ thin film

Bu [50] prepared nano $SrTiO_3$ power under the assisting of CTAB by sol–gel method and the thin film photoelectrodes were assembled. The performance of PEC anticorrosion to 304 SS was investigated under the irradiation of simulated daylight light source (LHX-Xe 300) with 300 W of light intensity. In this work, corrosive solution is 0.5 mol L^{-1} NaCl, electrolyte solution is 0.1 mol L^{-1} NaOH and 0.2 mol L^{-1} Na_2S in the photoelectric cell and the result is shown in Fig. 3–2. The photoelectrode coated with $SrTiO_3$ powders prepared in the absence of CTAB can pull the open circuit potential down to approximately −650 mV after light on. However the photoelectrode coated with $SrTiO_3$ powders prepared in the presence of CTAB can pull the open circuit potential down to approximately −700 mV after light on which presents better PEC anticorrosion performance.

$SrTiO_3$ films were prepared by Ohko [53] on an indium-tin oxide (ITO)-coated glass plate by a spray-pyrolysis technique. It was the first time to research the PEC cathodic protection performance of $SrTiO_3$ to carbon steel whose self-corrosion potential is more negative. Fig. 3-3(A) is the polarization curves of series materials. It can be seen that through the excitation of UV light, $SrTiO_3$ coating will produce photoexcited electrons, and then these photoexcited electrons will be transmitted directly to the carbon steel substrate to provide the protection of carbon steel. The potential of carbon steel could be pulled to approximately −770 mV by the $SrTiO_3$-coated ITO (*ca.* 1.5 mm thick) which was decreased about 220 mV compared with the self corrosion potential of the carbon steel.

In order to verify the PEC cathodic protection performance of the $SrTiO_3$ photoelectrode, the corrosion weight loss test was also carried out, and the result is shown in Fig. 3-3(B). A $SrTiO_3$ coating which is thinner than 1.5 μm may be enough to exhibit a practical PEC anticorrosion effect.

However, there are two problems when $SrTiO_3$ used as the material for the PEC cathodic protection. Firstly, it can only absorb the ultraviolet light because of the wide band gap 3.2 eV. On the other hand, the combination rate of photogenerated electron–hole pairs is high, in other words, the utilization rate of trapped photons is low. Therefore, in order to get a better application of $SrTiO_3$ in the field of PEC cathodic protection, it is necessary to solve these two problems.

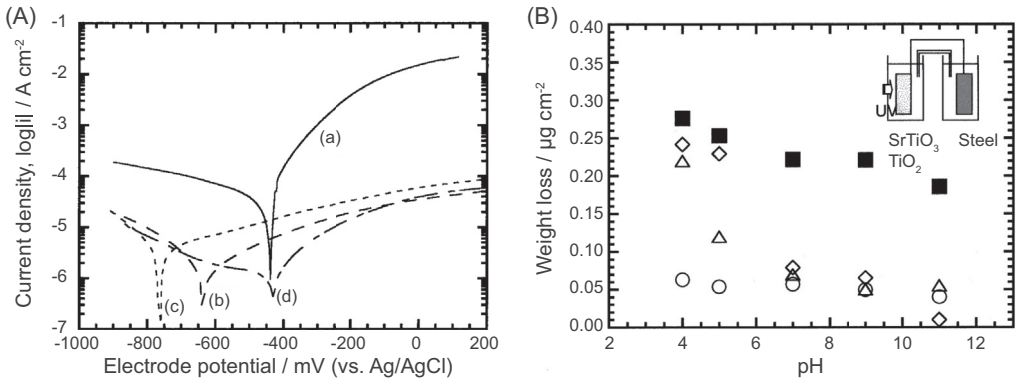

Fig. 3-3. **(A)** Polarization curves of (a) a carbon steel substrate in the dark, (b) an ITO electrode coated with $SrTiO_3$ (*ca.* 0.7 μm thick) under UV illumination, (c) an ITO electrode coated with $SrTiO_3$ (*ca.* 1.5 μm thick) under UV illumination, and (d) an ITO electrode coated with TiO_2 (*ca.* 1.2 μm thick) under UV illumination. The UV intensity was 10 mW cm^{-2}. Test solution: aerated 3 wt % NaCl (pH 5) at room temperature. **(B)** Amounts of iron dissolved for 1 h from carbon steel substrates in test solutions (50 mL) as functions of pH. The substrate was (■) not connected, or it was connected to the UV-irradiated (10 mW cm^{-2}) (△) $SrTiO_3$-coated ITO (*ca.* 0.7 μm thick), (○) the $SrTiO_3$-coated ITO (*ca.* 1.5 μm thick), or (◇) the TiO_2-coated ITO (*ca.* 1.2 μm thick) as illustrated in the inset. The carbon steel substrates were not illuminated. Test area was limited to 1 cm^2. The test solution was quiescent, aerated 3 wt % aqueous NaCl at room temperature.

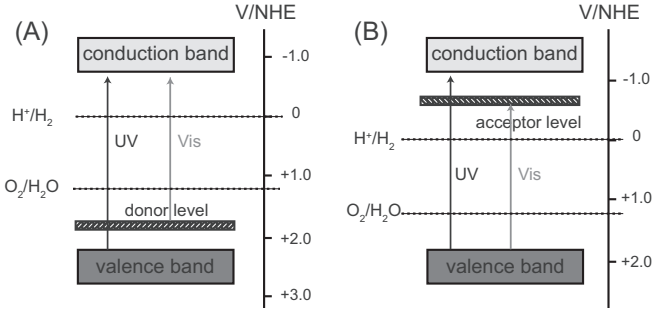

Fig. 3-4. Scheme of donor and acceptor level caused by metal doped.

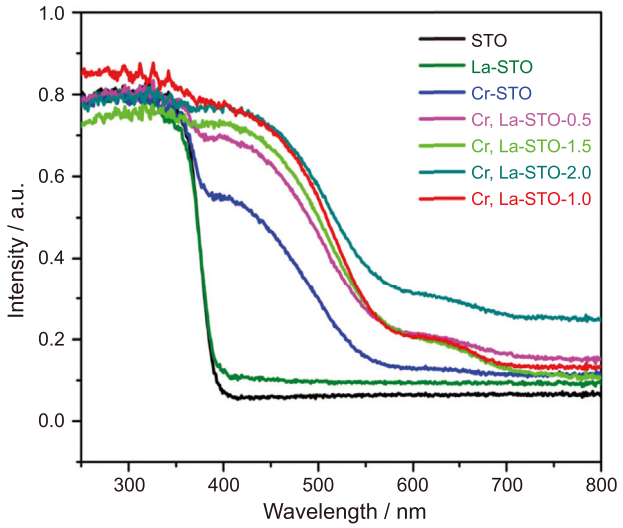

Fig. 3-5. UV–vis diffuse reflectance spectra of all the synthesized samples.

3.2. Doping $SrTiO_3$

3.2.1. Metal doping $SrTiO_3$

Leading a donor or acceptor energy level into a semiconductor band gap by metal doping is one of the most effective ways to extend the optical absorption threshold of semiconductors to the visible right region. Fig. 3-4 is the scheme of donor and acceptor level caused by metal doping. It can be seen from Fig. 3-4, whether the acceptor energy level or the donor energy level can effectively shorten the semiconductor band gap, so that the semiconductor can absorb and utilize the visible light. But for the semiconductor material used in the field of PEC cathodic protection, it is important to maintain the negative CB potential. Therefore, the doping energy level on the top of the valence band is more appropriate.

Cr [52,54–59], La [58–60], Rh [60,61], Sb [54], Fe [62] elements are often used to broaden the light absorption range of $SrTiO_3$. Liu et al. [55] prepared $SrTi_{1-x}Cr_xO_3$ (x = 0.00, 0.02, 0.05, 0.10) photocatalyst by solvothermal method. With the increase of the doped Cr, the hydrogen production activity under the visible light has been greatly improved, The absorption edge of Cr doped $SrTiO_3$ prepared by Tonda [56] is extended to about 600 nm, however, the absorption edge of Cr, La co-doped $SrTiO_3$ is extended to about 650 nm, as shown in Fig. 3–5, and the photocatalytic degradation performance has been greatly improved.

$SrTiO_3$ doped with Cr cations on different sites was studied by Wang et al. [57]. The results showed that the Cr cations doped at the Sr^{2+} site were all trivalent state (Cr^{3+}), while those doped at the Ti^{4+} site were mixed valent states (Cr^{3+} and Cr^{6+}). No matter which state Cr ions doped in $SrTiO_3$, its absorption of visible light has a very significant increase. As shown in Fig. 3-6(A), a new absorption edge appears at around 650 nm in either $(Sr_{0.95}Cr_{0.05})TiO_3$ or $Sr(Ti_{0.95}Cr_{0.05})O_3$, which could preliminarily be ascribed to the excitation from the occupied Cr 3d orbitals to Ti 3d orbitals. However it shows great difference in the photocatalytic activities of H_2 evolution between $(Sr_{0.95}Cr_{0.05})TiO_3$ and $Sr(Ti_{0.95}Cr_{0.05})O_3$. As shown in Fig. 3-6(B), the H_2 evolution rate over $(Sr_{0.95}Cr_{0.05})TiO_3$ (21 μmol/h) is more than 100 times that over $Sr(Ti_{0.95}Cr_{0.05})O_3$ (0.2 μmol/h). The empty Cr^{6+} level usually behaves as the trapping center for photoinduced electrons for its potential is lower than that for H_2 evolution. Thus, H_2 is not able to evolve over $Sr(Ti_{0.95}Cr_{0.05})O_3$. In contrast, the occupied Cr^{3+} level is located at a definite position (~1.0 eV) above O 2p, rendering

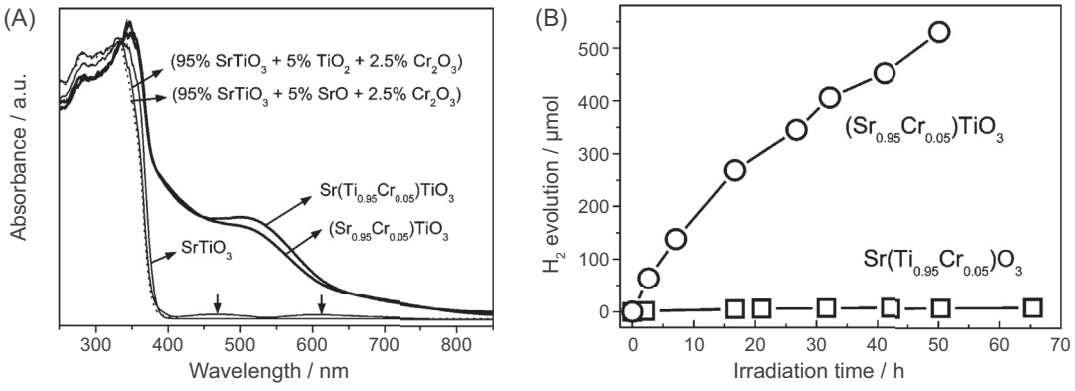

Fig. 3-6. **(A)** UV–vis diffuse reflectance spectra of $SrTiO_3$, $(Sr_{0.95}Cr_{0.05})-TiO_3$, $Sr(Ti_{0.95}Cr_{0.05})O_3$, and mixtures of (95 mol % $SrTiO_3$ + 5 mol %TiO_2 + 2.5 mol % Cr_2O_3) and (95 mol % $SrTiO_3$ + 5 mol % SrO + 2.5 mol % Cr_2O_3) at room temperature. **(B)** Photocatalytic H_2 evolution from the aqueous CH_3OH solution (50 mL CH_3OH + 220 mL H_2O) over Pt (0.4 wt%)-loaded $(Sr_{0.95}Cr_{0.05})TiO_3$ and $Sr(Ti_{0.95}Cr_{0.05})O_3$ powder (0.25 g) photocatalyst under visible light irradiation ($\lambda \geq 420$ nm). Light source: a 300 W Xe lamp (operated at 200 W).

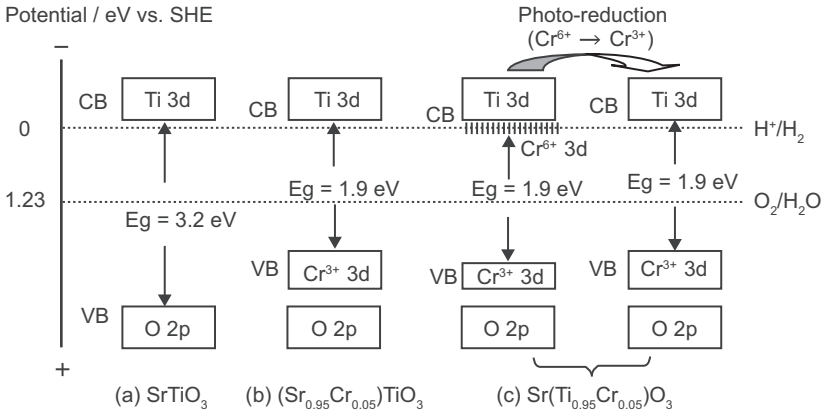

Fig. 3-7. Schematic band structures of (a) $SrTiO_3$, (b) $(Sr_{0.95}Cr_{0.05})TiO_3$, and (c) $Sr(Ti_{0.95}Cr_{0.05})O_3$ before and after photoreduction. The hexavalent Cr^{6+} was reduced to Cr^{3+} upon UV light irradiation.

the $(Sr_{0.95}Cr_{0.05})TiO_3$ to evolve H_2 under visible light irradiation.

The presence of Cr^{6+} doping energy level below the CB of $SrTiO_3$ is not only detrimental to enhance the PEC performance, but also harmful for PEC cathodic protection [56]. On the one hand, the doping energy level below the CB makes the CB potential of the semiconductor shift to the positive direction and makes photogenerated electrons reduction ability relatively decreasing, resulting in that the material cannot achieve the PEC cathodic protection effect on the metal whose self-corrosion potential is negative. On the other hand, the presence of Cr^{6+} doping level below the CB is widely considered to be the capture center of secondary recombination of photogenerated electrons and holes, and its existence inhibits the separation efficiency of photogenerated electron–hole pairs (Fig. 3-7).

3.2.2. Nonmetal doping $SrTiO_3$

Nonmetal doping is another effective methods to narrow the bandgap width of $SrTiO_3$. Compared with metal doping, nonmetal doping does not introduce new doping level, but the valence band will move to the negative direction to narrow the band gap of materials.

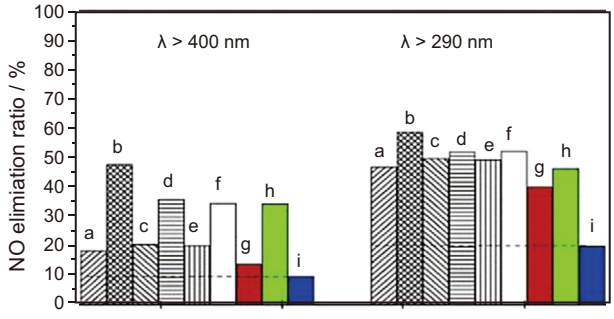

Fig. 3-8. The photocatalytic activity of various samples under irradiating light λ > 400 nm and ultraviolet light (λ > 290 nm). (a) As-ball milled with hexamethylenetetramine, (b) calcined (a) at 400 °C for 1 h, (c) as-ball milled with urea, (d) calcined (c) at 400 °C for 1 h, (e) as-ball milled with $(NH_4)_2CO_3$, (f) calcined (e) at 400 °C for 1 h, (g) $SrTiO_3$, (h) TiO_2(P-25), and (i) blank without sample.

Wang [63] prepared N doping $SrTiO_3$, in which hexamethylenetetramine, urea, and ammonium carbonate are used N source respectively. The absorption of visible light increased with nitrogen content doped in $SrTiO_3$ lattice increasing. They also tested the elimination rate of NO, as shown in Fig. 3-8, the photocatalytic activity of N doped $SrTiO_3$ was obviously improved. The value was about 3.5 and 1.4 times higher than those of pure $SrTiO_3$ and TiO_2 powder (Degussa P-25), as seen in Fig. 3-8 b, g and h.

Yu et al. [64] prepared Cr/N co-doping $SrTiO_3$ by sol–gel hydrothermal method based on the Cr doping $SrTiO_3$. As shown in Fig. 3-9, the band gap of Cr doping $SrTiO_3$ reduces to 2.5 eV, after N doping, the valence band potential of $SrTiO_3$ is raised up, and the band gap is further reduced to 2.4 eV. What's more, the Cr/N-codoped $SrTiO_3$ photocatalyst exhibits higher photocatalytic activities for hydrogen production than Cr-doped $SrTiO_3$, which can be attributed to that the Cr/N-codoped $SrTiO_3$ has smaller band gap and much less vacancy defects than Cr-doped $SrTiO_3$.

Nonmetal doping can effectively narrow the band gap of $SrTiO_3$, widen the range of light absorption, but for PEC cathodic protection, nonmetal doping method has not been attracted enough attention, and even the types of doped nonmetal elements have been limited, so the PEC cathodic protection of nonmetal doping $SrTiO_3$ still have a large space to increase the research.

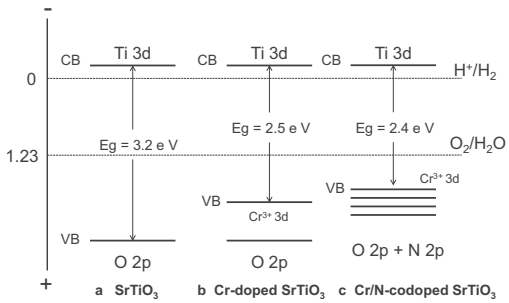

Fig. 3-9. The electronic band structures for (a) $SrTiO_3$, (b) Cr doped $SrTiO_3$ and (c) Cr/N-codoped $SrTiO_3$.

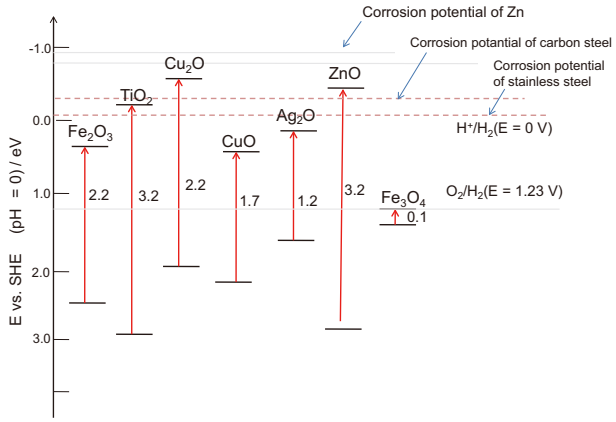

Fig. 3-10. The band structure of common semiconductor materials.

3.3. $SrTiO_3$ composite

It is one of the effective ways to inhibit the fast recombination of photogenerated electron–hole pairs by combining $SrTiO_3$ with other semiconductors. The two semiconductors with well-matched conduction and valence band can ensure that carriers efficiently transfer from one semiconductor to another. Cao et al. [65] prepared $SrTiO_3/TiO_2$ nanofiber by simple in-situ hydrothermal growth method. It was found that the tight coupling of $SrTiO_3$ and TiO_2 can effectively inhibit the recombination of photoinduced electron–hole pairs. Compared with pure TiO_2, the photocatalytic activity of $SrTiO_3/TiO_2$ heterostructure was greatly improved. The enhanced photocatalytic activity of $SrTiO_3/TiO_2$ nanofiber heterostructure could be ascribed to the enhanced charge separation derived from the coupling effect the TiO_2 and $SrTiO_3$ nanocomposite.

Choudhary et al. [66] prepared $CuO/SrTiO_3$ composite film with different thicknesses on the ITO glass substrate by sol–gel spin coating method. The results showed that the $CuO/SrTiO_3$ composite film exhibit excellent performance in the field of PEC water splitting. Maximum photocurrent density of 1.85 mA/cm^2 at −0.9 V (vs SHE) was exhibited by 590-nm-thick $CuO/SrTiO_3$ bilayered photoelectrode, which is approximately eight times higher than that for CuO and 30 times higher than that for $SrTiO_3$. The bilayered system offered increased photocurrent density and enhanced photoconversion efficiency, attributed to improved conductivity, which ameliorate separation of the photo-generated carriers at the $CuO/SrTiO_3$ interface and higher value of flat band potential.

Inspired by this work, Sharma et al. [67] built $SrTiO_3/Cu_2O$ p-n heterojunction film by depositing p-type Cu_2O and n-type $SrTiO_3$ on the ITO glass substrate through sol–gel spin coating and spray pyrolysis method respectively. It was found that the maximum conversion efficiency of 1.18% was exhibited by $SrTiO_3/Cu_2O$ heterojunction photoelectrode with overall thickness 454 nm as compared to $CuO/SrTiO_3$ heterojunction. The improved photoresponse of this photoelectrode may be attributed to the efficient separation of photogenerated charge carriers at the interface, reduction in resistance and improved light absorption ability.

These facts show that combining $SrTiO_3$ with other semiconductors can effectively improve the separation of photo-induced electrons and holes and can be well applied in the field of PEC. So, the application potential of $SrTiO_3$ in PEC cathodic protection should be excavated. Among all the semiconductor materials, TiO_2 has been extensively investigated for the purpose of PEC corrosion prevention of stainless steel and copper [25,68–70]. However, it is difficult to protect carbon steel from corrosion using TiO_2 thin film by the aforementioned PEC technique [53], because carbon steel has a relatively negative self-corrosion potential of about −0.6 V (vs. Ag/AgCl reference electrode) which is very close to the CB potential of TiO_2, as shown in Fig. 3-10.

A promising PEC material for corrosion protection of carbon steel is $SrTiO_3$. This material is a stable photocatalytic material with a similar band gap to TiO_2, while the CB potential is about 200 mV negative than that of TiO_2 [46,71,72]. Nevertheless, compared with TiO_2, $SrTiO_3$ nanocrystalline films exhibited only one-third photo-to-current conversion efficiency under the same conditions, as reported by Gratzel et al. [73].

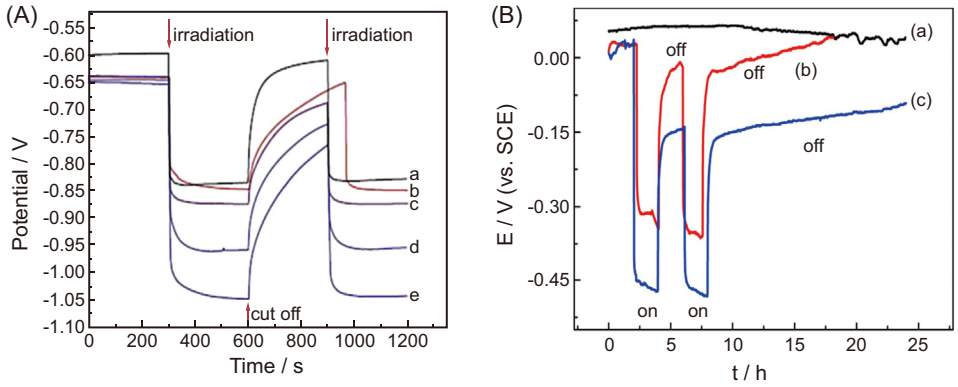

Fig. 3-11. (A) Photoinduced open circuit potential curve under interrupted illumination of white light of Q235 carbon steel coupled with $SrTiO_3/TiO_2$ nanotube array photoelectrode with a hydrothermal time of a) 0 h, b) 0.5 h, c) 1 h, d) 2 h and e) 5 h in $Sr(OH)_2$ solution, respectively. (B) Time evolution of the potential of 403 SS coupled to different photoanodes under illumination and dark conditions. (a) no coupling, (b) coupled to the TiO_2 film, (c) coupled to the $SrTiO_3/TiO_2$ film prepared by 1 h hydrothermal reaction.

On this basis, Zhang et al. [74] prepared TiO_2 thin film through the anodic oxidation method, and then further prepared $SrTiO_3/TiO_2$ heterojunction nanotube array thin film by hydrothermal growth. The result is shown in Fig. 3-11(A). $TiO_2/SrTiO_3$ nanotube array thin film with heterostructure has been demonstrated to be efficient for PEC corrosion protection of metals. The carbon steel, which has more negative self-corrosion potential than stainless steel, can be protected by coupling with the $TiO_2/SrTiO_3$ nanotube array thin film photoelectrode under the illumination of simulated sunlight.

Zhu et al. [75] prepared highly ordered TiO_2–$SrTiO_3$ nanotube arrays heterojunction by hydrothermal method. Compared with pure TiO_2 film, the composite film exhibits better separation efficiency of photogenerated electrons and holes and higher optical current conversion efficiency. As shown in Fig. 3-11(B), the thin film used as photoanode exhibits excellent cathodic protection that it could negatively shift the potential of 304 stainless steel to 480 mV in 0.5 mol/L NaCl solution.

In summary, the relative negative CB potential of $SrTiO_3$ makes it show great application prospect in the field of PEC cathodic protection. However, the research mainly focused on pure $SrTiO_3$ and $TiO_2/SrTiO_3$ composites. There is a few of research on the PEC cathodic protection focusing on metal and nonmetal doped $SrTiO_3$ or composite of $SrTiO_3$ with other semiconductors. It was found that doping elements or combining the semiconductors could effectively broaden the response range of light of $SrTiO_3$, and improve the separation of photogenerated electron–hole pairs. Thus, these modification methods should be employed to improve the PEC cathodic protection property of $SrTiO_3$ further.

4. Other PEC cathodic protection materials

4.1. PEC cathodic protection of ZnO photoanode

In recent years, ZnO has been widely used in the field of photochemistry, photocatalytic hydrogen production [76,77], photocatalytic degradation of pollutants [78,79], photocatalytic antibacterial [80] and other fields, because of its non toxicity, high efficiency, low cost and so on. In addition, ZnO is a kind of n-type semiconductor, and the CB potential is more negative than the corrosion potential of 304 SS, Q235 CS (As shown in Fig. 3-10), so it is a promising material for photoelectrochemical cathodic protection. Even though the photoelectric chemical properties of ZnO are better than these of TiO_2 in some extent, its chemical stability is not better than that of TiO_2. So the applications of ZnO in the field of PEC cathodic protection are less than TiO_2. However, if the stability of ZnO is solved, it will be a potential material for PEC cathodic protection.

4.1.1. PEC cathodic protection electrode of pure ZnO

Sun et al. [81] prepared ZnO photoanode and researched the PEC cathodic protection of ZnO photoanode for Q235 CS and 304 SS. As shown in Fig. 4–1, the research results showed that the ZnO photoanode could not provide a PEC cathodic protection for Q235 CS, but just for 304 SS. Although the CB potential of ZnO is slight negative than the self-corrosion potential of Q235 CS, the productive rate of photogenerated electrons was much less than the electrons loss rate of Q235 CS in NaCl corrosion solution, thus the ZnO photoanode cannot provide a PEC cathodic protection for it. Combining ZnO with other materials to form a heterojunction structure is a considerable method to improve the separation efficiency of photogenerated charges and enhance the stability of ZnO photoanode.

4.1.2. PEC cathodic protection electrode of composited ZnO

The cathodic protection effect of ZnO loaded In_2S_3 on 304 SS electrode was studied by Jing et al. [82]. Fig. 4-2 (A) showed the PEC cathodic protection performance of In_2S_3/ZnO compound photoanode for 304 SS. It can be seen that the 304 SS electrode coupled with the photoelectrode showed a rapid potential drop with illumination, indicating that the electrons in the valence band of In_2S_3 were excited to its CB and subsequently transferred to the coupled 304 SS, leading to a potential drop of the 304 SS electrode under visible light. Fig. 4-2 (B) showed the stability of PEC cathodic protection performance for 304 SS. They found that the 304 SS remained stable in visible light irradiated after 1 h, indicating that the In_2S_3/ZnO composite could provide a very stable cathodic protection for the 304 SS under visible light irradiation.

Xu et al. [83] also synthesized TiO_2/ZnO by this method and achieved the low energy loss from TiO_2 to ZnO by promoting the rapid charge separation between TiO_2 and ZnO, whether in dark state or light the composites have a more negative OCP than pure ZnO (shown in Fig. 4-3 (A)). At the same time, it can be seen from the EIS diagram that the composite material has a smaller arc radius than that of pure ZnO in dark state or illumination, indicating that the recombination efficiency of electrons and holes of TiO_2/ZnO is obviously smaller than that of pure ZnO.

Although the ZnO has poor stability and less application in photoelectrochemical cathodic protection, Sun et al.'s research showed that the conduction potential of ZnO is more negative than carbon steel, stainless steel corrosion potential, so it can be used for photoelectrochemical cathodic protection. And the method of doping and semiconductor recombination would broaden the absorption range of ZnO and reduce the recombination efficiency of electron hole to further improve the photoelectrochemical cathodic protection performance of ZnO in the visible light range.

4.2. PEC cathodic protection of graphite carbon nitride ($g\text{-}C_3N_4$)

As a typical metal-free semiconductor, graphitic carbon nitride ($g\text{-}C_3N_4$) with a bandgap width 2.7 eV, has been wildly applied in photocatalytic water splitting [84], photocatalytic degradation of organic pollutants [85] and photosysthesis [86,87] etc. Recently, application of graphitic carbon nitride ($g\text{-}C_3N_4$) in the field of PEC cathodic protection has attracted

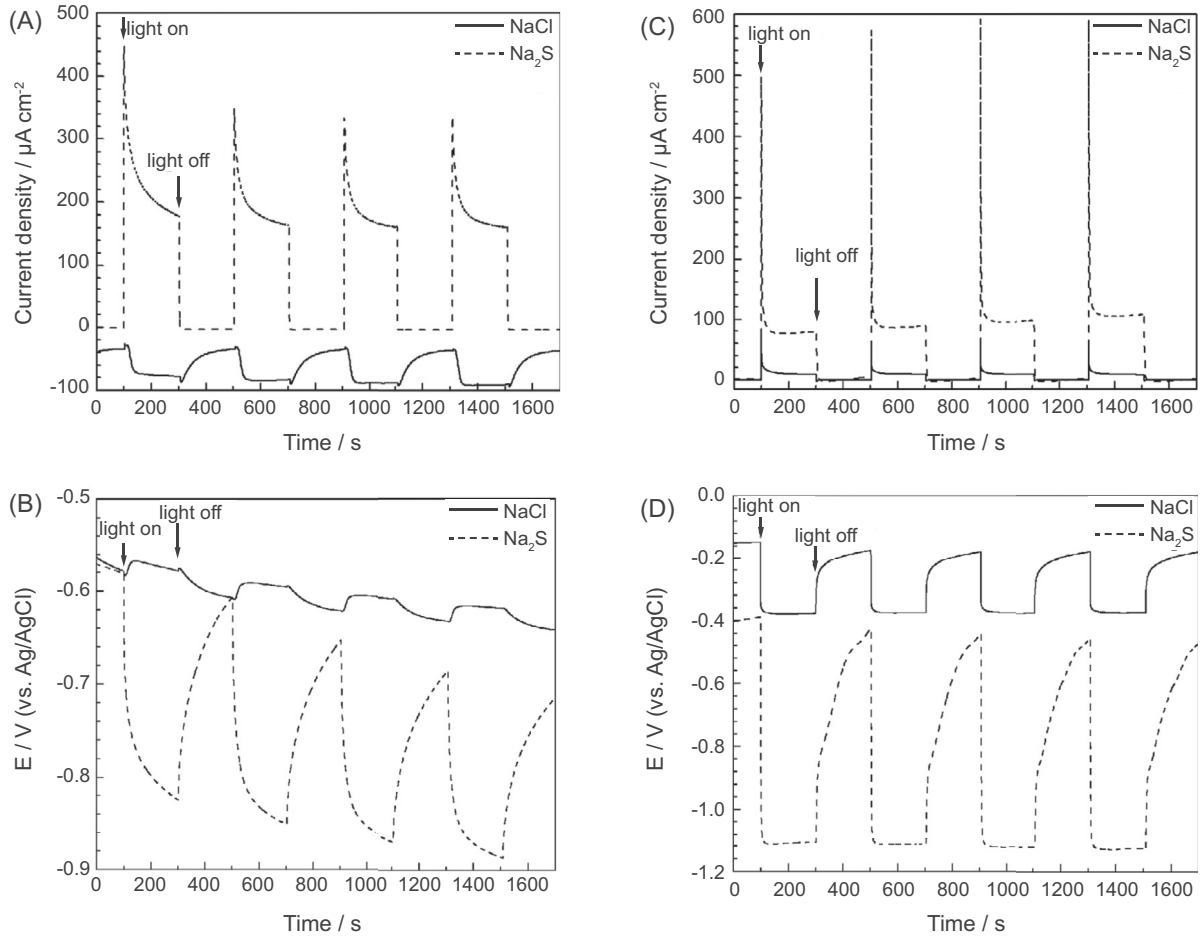

Fig. 4-1. (A) The photoinduced current densities between ZnO thin-film photoelectrode and Q235 CS electrode and (B) the photoinduced OCP variations of the coupled ZnO thin-film photoelectrode with Q235 CS electrode (C) The photoinduced current densities between ZnO thin-film photoelectrode and 304 SS electrode and (D) the photoinduced OCP variations of the coupled ZnO thin-film photoelectrode with 304 SS electrode under intermittent white light illumination. The solid lines are the results obtained by immersing the ZnO thin-film photoelectrode in 3.5% NaCl solution in the photoelectricity cell, while the dotted lines are the results obtained by immersing the ZnO thin-film photoelectrode in 0.1 mol/L $Na_2S + 0.2$ mol/L NaOH solution in the photoelectricity cell. For both conditions, the Q235 CS electrode was immersed in 3.5% NaCl solution in the corrosion cell.

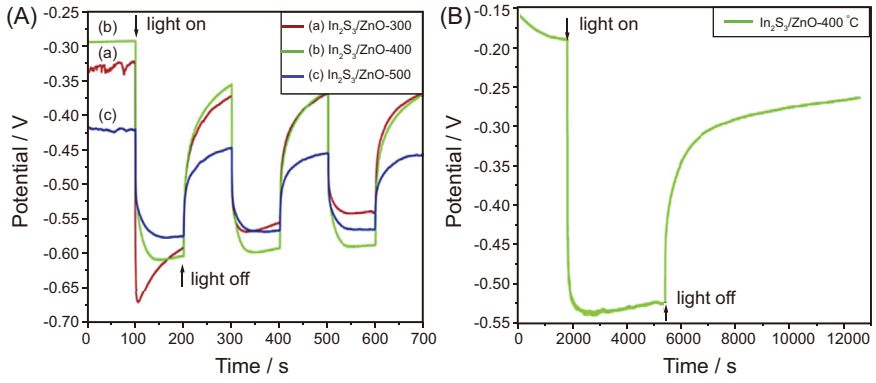

Fig. 4-2. (A) Variations of the open circuit potential of the galvanic coupling of the 304 SS electrode and the thin-film photoelectrodes prepared with the In_2S_3/ZnO NRA composites sintered at 300 (a), 400 (b) and 500 °C (c) under intermittent visible light illumination. (B) Changes in the open circuit potential of the 304 SS electrode coupled with the thin-film photoelectrode prepared with the In_2S_3/ZnO NRA composite sintered at 400 °C under 1 h visible light illumination and subsequently 2 h in the dark.

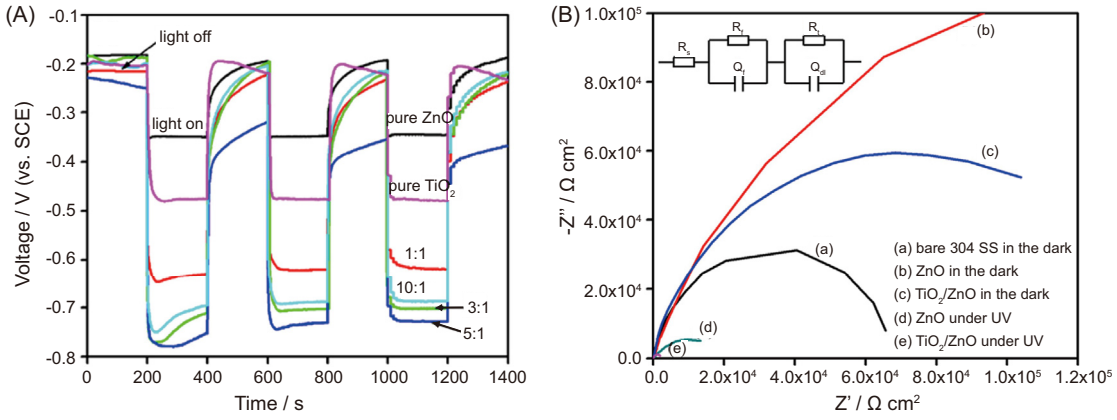

Fig. 4-3. (A) Variation of the open circuit potential (B) Nyquist plots of the samples in the absence and presence of UV light and for bare 304 SS electrode in 3.0% NaCl solution. The inset figure is the corresponding equivalent circuit.

more and more attentions. Zhang et al. [88] indicated that g-C_3N_4 has a more negative CB potential with a rectifying characteristic similar to that of n-type semiconductor. Wang et al. [84] calculated the energy band potential of g-C_3N_4 by the density functional theory and found that the CB potential of g-C_3N_4 is −1 V (vs. NHE), meanwhile, the valence band potential is enough to oxidize the OH^- from the water to oxygen. These physical characteristics demonstrated that g-C_3N_4 is a promising semiconductor used in the field of PEC cathodic protection of metals.

Bu et al. [89] firstly explored the feasibility of g-C_3N_4 for PEC cathodic protection of 304 stainless steel, as shown in Fig. 4-4, the OCP variations illustrated that the migration velocity of the photo-induced electrons to the 304 SS electrode was higher than the consumption rate of the electrons on the 304 SS electrode surface by the oxygen reduction in the electrolyte solution, so that electrons could accumulate on the 304 SS electrode and polarize it to a much more negative potential, allowing 304 SS to become cathodic protection by the g-C_3N_4 thin-film photoanode. Except providing PEC cathodic protection for 304 SS, the g-C_3N_4 thin film could also provide physical protection as a barrier coating for it.

Although g-C_3N_4 shows great potential for PEC cathodic protection, there is still a significant problem needs to be addressed. The photogenerated holes produced by g-C_3N_4 could not oxidize water to oxygen easily because of its relative low valence band potential (1.3 V vs. NHE), meaning that the anodic depolarization process of the holes photoinduced by g-C_3N_4 does not occur easily in the commonly used corrosion electrolyte systems, for example 3.5% NaCl, where water is the only hole scavenger. Therefore, in order to improve the applicability of g-C_3N_4 in the field of PEC anticorrosion effect on metal, g-C_3N_4 must be modified to increase the

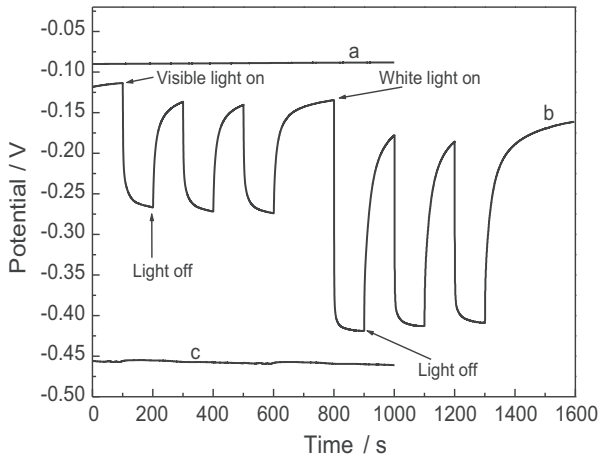

Fig. 4-4. Changes in the OCPs of (a) the 304 SS electrode in 3.5% NaCl, (b) the 304 SS electrode coupled with the g-C_3N_4 thin-film photoelectrode under conditions of visible and white light switched on and off, and (c) the g-C_3N_4 thin-film photoelectrode in 0.1 M Na_2S + 0.2 M NaOH in the dark.

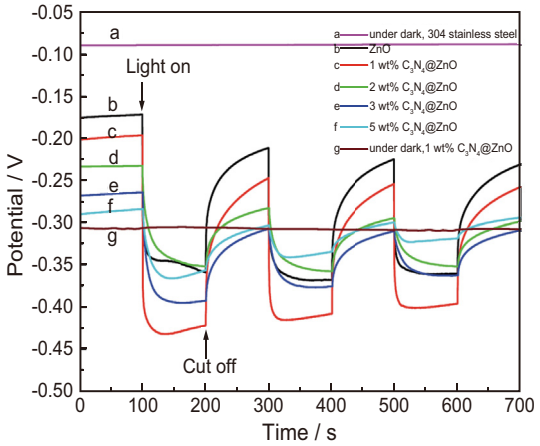

Fig. 4-5. Open circuit potential of the Galvanic couple of 304 stainless steel with ZnO (curve b); 1 wt% C_3N_4@ZnO quasi-shell−core composite (curve c); 2 wt% C_3N_4@ZnO quasi-shell−core composite (curve d); 3 wt% C_3N_4@ZnO quasi-shell−core composite (curve e); 5 wt% C_3N_4@ZnO quasi-shell−core composite (curve f) under white light switched on and off intermittently. Curve a is the open circuit potential of 304 SS electrode and curve g is that of 1 wt% C_3N_4@ZnO quasi-shell−core composite photoelectrode in the dark in 3.5 wt% NaCl solution.

depolarization capability of the holes generated by g-C_3N_4 photoelectrode in the process of the PEC reactions.

Bu et al. [90] further extended applications of the C_3N_4 in the field of PEC cathodic protection. He prepared different ratios of C_3N_4@ZnO shell–core structure of composite materials, to study the PEC cathodic protection effect. As shown in Fig. 4-5, when the loading amount of C_3N_4 was 1 wt%, the composite exhibited the best PEC cathodic protection performance, and a thin protective layer of C_3N_4 was covered on the surface of ZnO to form an interface heterojunction electric field, effectively improving the photogenerated electron–hole separation efficiency and the PEC cathodic protection property for 304 SS.

Sun et al. [91] prepared quasi-shell–core nanocomposite C_3N_4@In_2O_3 and applied it on photoelectrochemical cathodic protection. As shown in Fig. 4-6, the photoinduced OCP and current density results indicate that the 3 wt% C_3N_4@In_2O_3 quasi-shell–core composite can provide the best PEC cathodic protection for the coupled 304 SS. The heterojunction field at the interface between C_3N_4 and In_2O_3 effectively promotes the separation of photogenerated electrons and holes and enhances the lifetime of photogenerated electrons and accelerates the interfacial reaction, allowing more photogenerated electrons to migrate to the 304 SS substrate, to suppress the dissolution of the 304 SS in the anode region.

In order to optimize the electron transport capacity between C_3N_4 and semiconductor materials, Bu et al. [92] prepared O-doped C_3N_4 by hydrothermal oxidation method, and used the surface oxidation groups on O-C_3N_4 to attach with the surface hydroxyl residues on TiO_2 nanoparticles. As shown in Fig. 4-7, it was found that the photoinduced current density of the prepared O–C_3N_4@TiO_2 composite increased greatly when the ratio of the O–C_3N_4 added amount increases to 3 wt%, which is approximately two times higher than that of pure TiO_2. While, the photoinduced current density of the 3 wt% C_3N_4@TiO_2 composite is only slightly higher than that of pure TiO_2. This phenomenon contributed to the interface bridge bonds formed between O–C_3N_4 and TiO_2 that decline the charge transfer resistance between them, resulting in higher photo to electric conversion efficiency and higher PEC cathodic protection performance for metal.

Because of the negative enough CB potential of g-C_3N_4, it shows great research potential in the field of PEC cathodic protection. To date, the work on PEC cathodic protection for g-C_3N_4 based materials has not attracted enough attention. Therefore, it is very interesting to develop more efficiency PEC cathodic protection photoanodes on g-C_3N_4 based materials. Especially, the electron mobility of g-C_3N_4 and its anodic depolarization energy barrier of the photogenerated holes should be improved further.

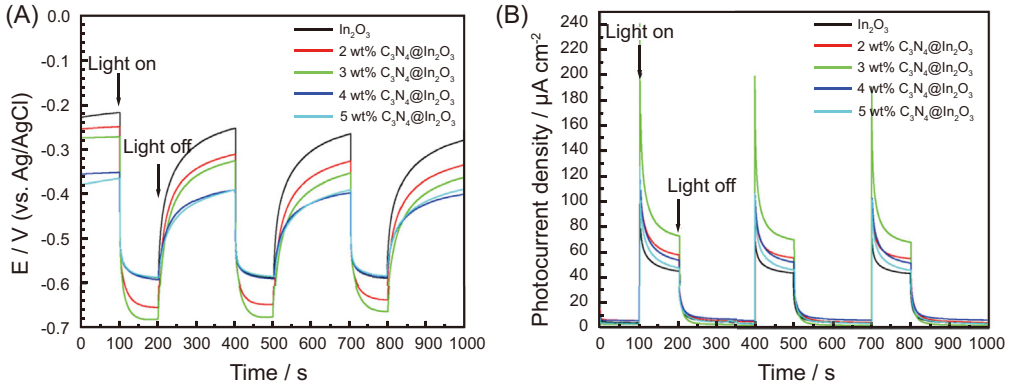

Fig. 4-6. (A) The photoinduced OCP variations of the coupled thin-film photoelectrode with 304 SS electrode, (B) the photoinduced current densities between the prepared thin-film photoelectrode and the 304 SS electrode and under intermittent visible light on and off.

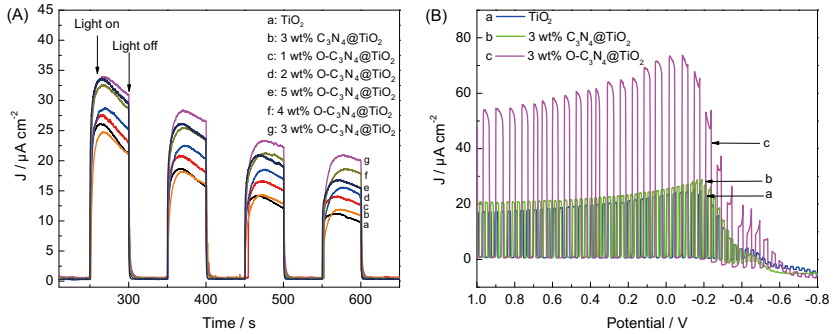

Fig. 4-7. (A) Variations in current densities at a 0 V bias potential (vs SCE) with time for the photoelectrodes prepared by TiO_2, 3 wt% C_3N_4@TiO_2 and O–C_3N_4@TiO_2 with different O–C_3N_4 adding ratios under intermittent white light illumination. (B) The photoinduced volt-ampere characteristic curves of TiO_2, 3 wt% C_3N_4@TiO_2 and 3 wt% O–C_3N_4@TiO_2.

5. Photoelectric energy storage and PEC cathodic protection dual-function electrodes

Traditional TiO_2 photoanode just can provide PEC cathodic protection for metals under light irradiation. In order to keep its continual work in aphotic situation, suitable energy storage materials should be composited on the TiO_2 photoanode, and the operation mechanism of this system should also be figured out. This new technology is consisted of a PEC cathodic protection system and an energy storage system. During this system working, a part of photogenerated electrons in the semiconductor can transfer to the metal to provide the cathodic protection for it. Meanwhile, excessive amounts of photogenerated electrons are stored by the energy storage material system, then released to the metal in the aphotic conditions subsequently, and thus provide a continued protection for the metal.

Furthermore, high recombination rate of photogenerated carriers in pure TiO_2 coating can be inhibited by coupling another electron-stored semiconductor material to form a II-type heterojunction structure. Thus, TiO_2-electron storage semiconductor system possesses great practical application potential in the field of PEC cathodic protection for metal.

In this system, for the electron storage semiconductor, the reversible redox property is needed. In addition, its CB potential should locate between the CB potential of photoelectric functional semiconductor and the self-corrosion potential of the protected metal. So, the characteristics required for the electron storage materials are as the following: (1) redox activity; (2) more positive redox potential than the conduction band potential of the employed semiconductor (the oxidized form of the electron pool should accept electrons from the irradiated semiconductor); (3) more negative redox potential than the self-corrosion potential of the metal; (4) poor oxidizability of the reduced form by ambient oxygen; (5) stability during repeated redox cycles. It was found that the conduction band potentials of WO_3, CeO_2 and SnO_2 were more positive than that of TiO_2, and more negative than the corrosion potential of stainless steel also [68–70]. So, they have been used in PEC cathodic protection field widely.

5.1. WO_3–TiO_2 composite PEC cathodic protection electrodes

Based on this theory, WO_3–TiO_2 composite overlayer has been coated on 304 stainless steel substrates [68,93]. Among them, TiO_2 served as PEC cathodic protection material, and WO_3 coating was used as an energy storage material. As shown in Fig. 5-1, the electrons in the VB can be excited to the CB of the semiconductor under the light irradiation with the appropriate wavelength. Excited electrons are injected into the protected metal, which makes its potential more negative than the self-corrosion potential of the metal. Additional electrons are received by the connected electron pool (WO_3). When the WO_3 receives the photogenerated electrons from TiO_2, the M^+ in the electrolyte will react with it to form M_xWO_3 (M = H or Na). Hence, WO_3 will be reduced to a tungsten bronze-type composite (M_xWO_3; M = H, Li, Na, etc.; $x \leq 1$). As a result, the photogenerated electrons can be stored as a reduction energy.

In 3 wt% NaCl aqueous solution with pH = 5, the WO_3 coating on the surface of the 304 stainless steel substrate was charged with the TiO_2 coating irradiated with the ultraviolet light and then forming a blue composite, which resulted in a decrease in reflectance. In the dark, a reverse reaction would take place when the released electrons were transported to the substrate. The electrons which were stored in the charged WO_3 coating electron pool, were injected into the protected metal, thus the coating still has the effect of preventing metal corrosion. The charge–discharge cycles can be repeated and showed the same effect on PEC cathodic protection for WO_3–TiO_2 composite coating. The transition of electron is likely owing to that W element has a multivalent state. The photogenerated electrons would get energy when the surface of the TiO_2 coating is irradiated by ultraviolet light, and shift to the conduction band, leaving holes in the valence band. Since the band energy of WO_3 is lower than that of TiO_2, the photogenerated electrons can be injected into the conduction band of WO_3, leaving the photogenerated holes in the valence band of TiO_2, and the reaction took place as shown in Equations ((5-1)–(5-3)). Thus, the photogenerated electrons and holes are effectively separated. In the dark state, M_xWO_3 is

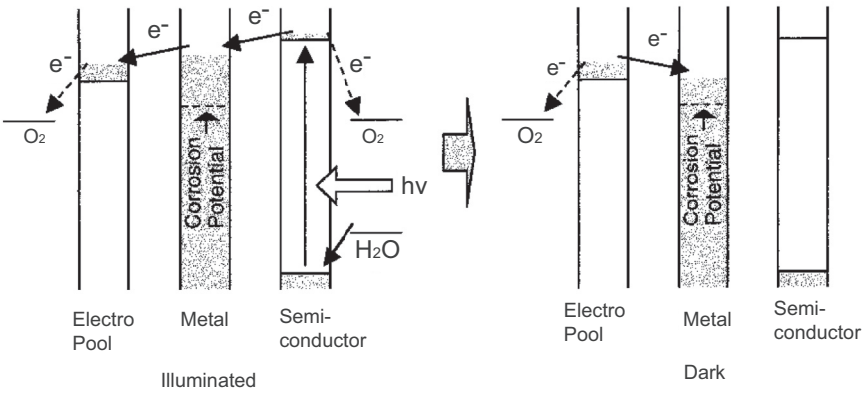

Fig. 5-1. Mechanism of a PEC anticorrosion system with an energy storage ability.

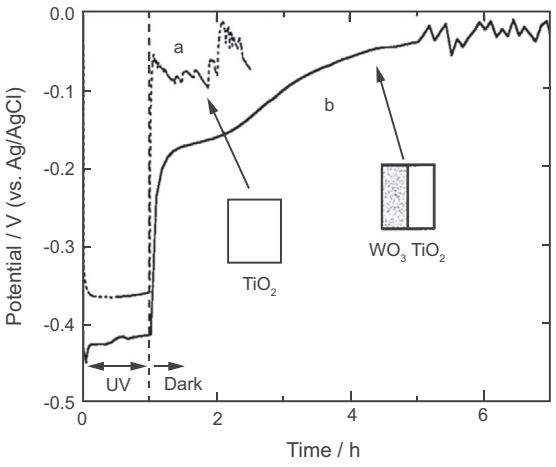

Fig. 5-2. Changes in the potential of a typical 304 stainless steel (1.75 cm^2) coated with TiO_2 (a) and that coated with TiO_2 and WO_3 (single coating) (area, 50% each) (b) in an air saturated 3 wt% NaCl solution, pH = 5. TiO_2 was irradiated with UV light for the first 1 h.

oxidized to WO_3 by the dissolved oxygen in the solution, providing PEC cathodic protection, as shown in Equations ((5-4)–(5-6)). As seen in Fig. 5-2, after irradiated with UV light for 1 h, the coupling WO_3–TiO_2 coating can provide the PEC cathodic protection in the dark for 5 h continuously.

$$TiO_2 \xrightarrow{UV} TiO_2^*\left(e^- + h^+\right) \quad (5-1)$$

$$2H_2O + 4h^+ \rightarrow O_2 + 4H^+ \quad (5-2)$$

$$WO_3 + xe^- + xNa^+ \rightarrow Na_xWO_3 \quad (5-3)$$

$$O_2 + 4H^+ + 4e^- \rightarrow 2H_2O \quad (5-4)$$

$$O_2 + 2H^+ + 2e^- \rightarrow H_2O_2 \quad (5-5)$$

$$O_2 + e^- \rightarrow O_2^-. \quad (5-6)$$

Hyunwoong et al. [94] further analyzed the charge/discharge process of TiO_2/WO_3 composite photoanode during the PEC cathodic protection process. Firstly, a charge separation occurred in TiO_2 and the electrons were accumulated under irradiation for several seconds. Secondly, WO_3 slowly absorbs photogenerated electrons generated by TiO_2 in order to charge. This process would last for several hours. Thirdly, while the light source was turned off, TiO_2 discharged rapidly in a few seconds. Fourthly, the slow discharge process of WO_3 would last for several hours. Finally, when all the electrons were reacted at the solid–electrolyte interface, the whole process would end.

In order to enhance the photoelectron storage capacity of the TiO_2/WO_3 composite photoanode, Ngaotrakanwiwat et al. [95] studied PEC cathodic protection and energy storage performance of WO_3–TiO_2 coating and phosphotungstic acid (PWA)–TiO_2 which prepared by spin coating method, in aqueous 3 wt% NaCl solution for the carbon steel electrode. The charging processes of the reaction are shown in Equations ((5-7) and (5-8)):

$$PW_{12}O_{40}^{3-} + xe^- + xM^+ \leftrightarrow M_xPW_{12}O_{40}^{3-} \quad (5-7)$$

$$WO_3 + xe^- + xM^+ \leftrightarrow M_xWO_3 \quad (5-8)$$

$M = H, Li, Na, etc.$

Corresponding results found that the charge capacities of WO_3–TiO_2 and PWA-TiO_2 coatings were 537 and 203 μC/cm^2, respectively. This phenomenon was owing to the larger particles size of PWA, which made the WO_3 charging reaction more easily. However, the discharge process of PWA-TiO_2 system was much slower than that of WO_3–TiO_2 system, as seen in Fig. 5-3. The PWA-TiO_2 system could provide longer time to protect the metal after cutting off the light. So it is more suitable for PEC cathodic protection applications.

Except the liquid-phase environment, WO_3–TiO_2 coating can also play a role in the atmosphere environment. Pailin et al. [96] studied the apparent quantum efficiency, maximum storage capacity and specific capacity of the coupled WO_3–TiO_2 coating by optimizing the coating composition, adjusting the incident light intensity and the coating thickness. It was found that the initial charge rate and the apparent quantum yield increased with the increasing of W/Ti ratio, and it was a promising system to protect the metal in the atmosphere environment.

5.2. SnO_2–TiO_2 composite PEC cathodic protection electrodes

Sn also exists a multi-valence state (+2, +4), and possesses higher carrier conductivity than WO_3. Therefore, the SnO_2–TiO_2 photoanode would be likely to more efficient than the WO_3–TiO_2 photoanode for PEC cathodic protection and electrons storage [69,97].

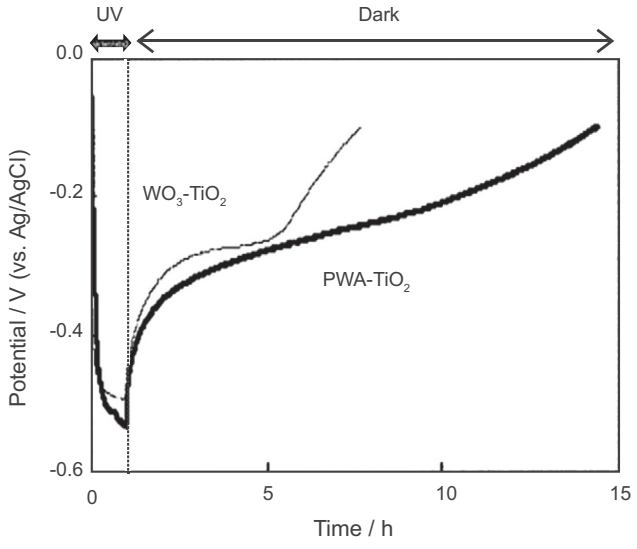

Fig. 5-3. Potential changes of the PEC charged (1 mW/cm^2, 1 h)PWA-TiO_2 and WO_3–TiO_2 Films in 3 wt% aqueous NaCl.

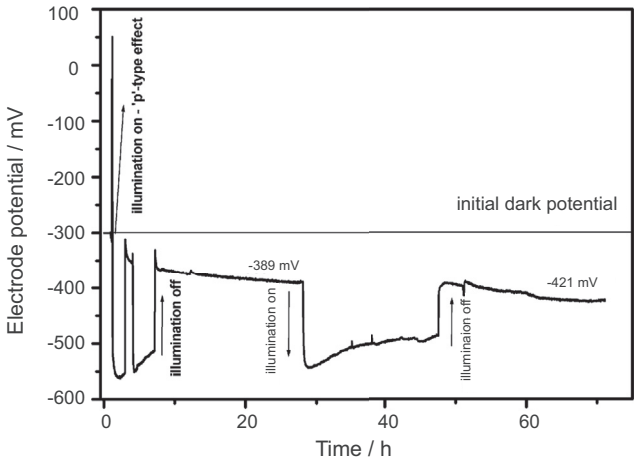

Fig. 5-4. Time dependence of the electrode potential for ITO coated with SnO_2–TiO_2 on exposure to UV illumination in deaerated atmosphere.

Subasri et al. [69] studied the PEC cathodic protection performance of the TiO_2/SnO_2 composite photoanode for metals. The results showed that when the composite ratio located at 1:1, the negative shift of the photogenerated potential and the photogenerated current reached the maximum. The cathodic protection of TiO_2–SnO_2 composite electrode irradiated for 4 h could be sustained for 64 h in dark [97], as shown in Fig. 5-4.

The energy storage effect of the system is partly due to the injection of photogenerated electrons into the SnO_2 particles under the light illumination, which is captured by the holes of the SnO_2 particles (5-9) [69]:

$$SnO_2 + e^- \rightarrow SnO_2(e_t) \quad (5-9)$$

The trapped electrons (e_t) can be easily re-injected back on the CB, when the CB is like a shallow trap. This kind of analysis is commonly used to explain electrochromic and photochromic behavior on SnO_2 thin films.

On the other hand, SnO_2 as an energy storage material, can be inserted in the H^+ from the electrolyte (5-10):

$$xH^+ + SnO_2 + xe^- \rightarrow H_xSnO_2 \quad (5-10)$$

The above reaction is carried out with excess electrons emitted from the TiO_2 under the light illumination. Reverse reaction occurs in the dark, maintaining a sufficiently negative potential after the illumination is stopped.

5.3. CeO_2–TiO_2 composite PEC cathodic protection electrodes

Due to that the conduction band potentials of WO_3 and SnO_2 are relatively positive, the reduction capacity of the photogenerated electrons produced by TiO_2 is reduced after compositing it with SnO_2, so that the PEC cathodic protection property for the metal is also reduced. Therefore, it is of great significance to develop some electron storage semiconductors with negative conduction band potential to combine with TiO_2. Raghavan et al. [70] prepared a CeO_2–TiO_2 electrode on a copper substrate by a sol–gel method and observed the morphology of the ceria nanoparticles by using a high-resolution transmission electron microscope, the results are shown in Fig. 5-5(A). Further results showed that the potential of the stored CeO_2–TiO_2 electrode is more negative than that of the Sb-SnO_2–TiO_2 electrode, as shown in Fig. 5-5(B) due to the more negative CB potential of CeO_2. After cutting off the light, the stored electrons by Ce^{4+} in-situ reduction would be re-released to extend the cathodic protection for the metal.

Except the direct combination of CeO_2 and TiO_2, Li et al. [28] prepared a Ce-doped TiO_2 layer on the surface of 316L stainless steel by sol–gel method, and found that the doped thin film could provide PEC cathodic protection for 316L SS substrate, and also slowed down the corrosion speed of 316L SS after cutting off the light.

5.4. Porous structured TiO_2 photoanodes

Except combining with some semiconductors with capacitive capacity, correlative researches suggested that some TiO_2 films with special porous structure have the effect of delay protection on the metal after cutting off the light source. Li et al. [30] prepared a TiO_2 nanotube array layer on the Ti foil surface by anodic oxidation method. The corresponding SEM

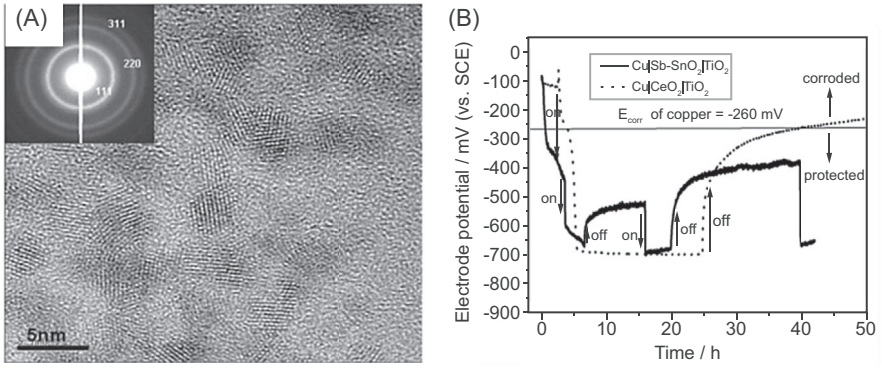

Fig. 5-5. (A) HRTEM image of nanoceria particles (with the size of 2–5 nm). (Inset shows the SAED pattern indicating the fluorite structure of nanoceria sample.) (B) Time evolution of electrode potential and its response to UV illumination compared with $Cu/CeO_2/TiO_2$ and $Cu/Sb\text{-}SnO_2/TiO_2$.

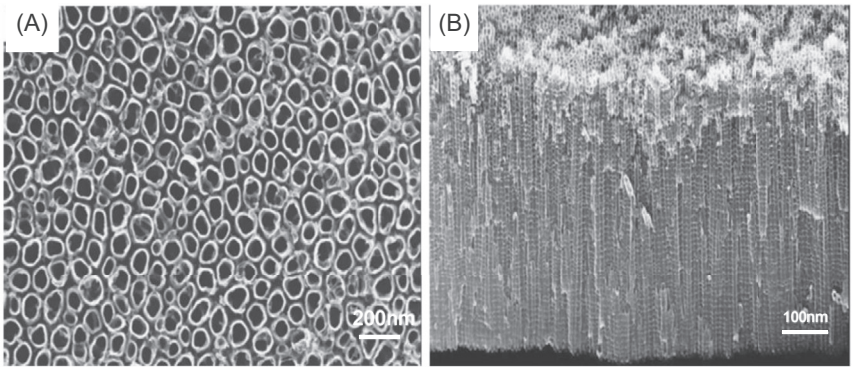

Fig. 5-6. Typical SEM images of the (A) top and (B) cross-sectional views for the N-doped TiO_2 nanotubular layers on Ti substrate.

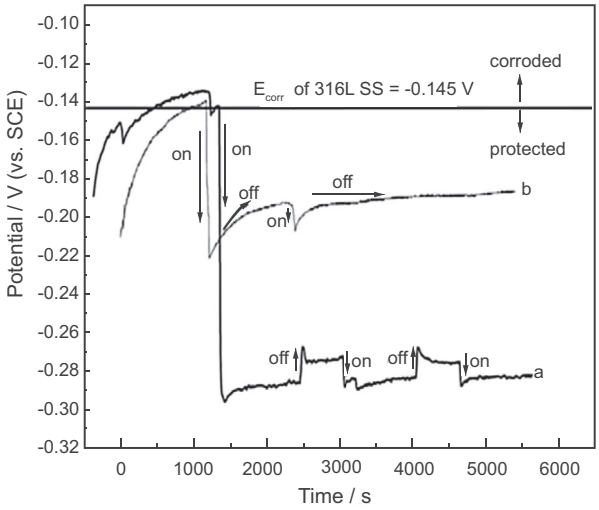

Fig. 5-7. Time dependence of OCP for 316L SS coupled with the TiO_2 nanotube layers and nanoparticle films under dark and illumination conditions. A comparison of the shift of the OCP of 316L SS coupled with the undoped TiO_2 nanotube (curve a) and TiO_2 nanoparticle films (curve b) electrodes exposed to UV illumination and in dark conditions.

image is shown in Fig. 5-6. It was found that the TiO_2 nanotube array with a thickness of about 500 nm and a diameter of about 90 nm was formed on the surface of the Ti substrate.

The corresponding PEC cathodic protection results are shown in Fig. 5-7. It can be seen that the TiO_2 nanotube rapidly generates the photoresponse under the irradiation of UV light and the potential stabilizes at −300 mV, which is effective for the cathodic protection of the stainless steel electrode. The dark state protection can maintain for several hours after 17 min illumination, which is mainly owing to the unique porous nanostructure of TiO_2 nanotubes which has a good storage capacity for photogenic electron−holes.

In order to improve the performances of the PEC cathodic protection and time-delay protection of TiO_2 nanotube arrays, Li et al. [20] prepared a highly ordered TiO_2 nanotube array by a two-step anodic oxidation process, as shown previously in Fig. 2-7. The TiO_2 nanotube structure obtained by the two-step anodic oxidation method can improve the photoelectric conversion efficiency remarkably. In addition, the negative shift of the electrode potential can be maintained for several hours even the illumination is cut off.

The above mentioned results show that TiO_2 films with special nanostructures can improve the photoelectrochemical cathodic protection performance for metals. Meanwhile this highly ordered structure possesses a very good storage capacity for the photogenerated electron−hole pairs. The photogenerated electron is released to the metal after cutting off the light thus providing time-delay cathodic protection. Therefore, it is very important to optimize the microstructure of TiO_2 by adjusting its morphology.

The energy storage material coupled with the photoelectric conversion material can solve the problems of continued protection of metal in the aphotic environment. At present, the charging efficiency and the continued protection property after cutting off the light of the photoanode need to be improved further.

6. Surface coating technology

Coating on metal plays the core function for metal anticorrosion, because it can isolate corrosion induced agent such as oxygen and water to contact with metal. So, if a semiconductor thin film coated on the surface of metal and keep a well contact, it not only provides PEC cathodic protection to the metal under sunlight illumination, but also plays an important role to isolate the corrosion factors with the metal, so that provides a dual protection system for the metal. To date, few coating technologies have been employed to fabricate semiconductor thin film on the metals directly, and we summarized them as follows.

6.1. Sol−gel method

Shen et al. [25] prepared a TiO_2 nanofilm on 316L SS by dip coat the TiO_2 sol on it and then annealing at 450 °C. Photoinduced OCP change and electrochemical impedance spectroscopy (EIS) results indicated that the surface coated TiO_2 nanofilm could provide a considerable PEC cathodic protection property for 314L SS, meanwhile the solid−liquid interface resistance was increased greatly after TiO_2 nanofilm

coating, meaning that a physical isolation protection could be provided to the 314L SS also.

In traditional metal anticorrosion coating, Cr element is widely added, because Cr can passivation the surface of the steel, to enhance the anticorrosion performance of the coating. Li et al. [27] prepared a Cr-doped TiO_2 nanolayer on the surface of 316L SS, and found that the Cr-doped TiO_2 nanolayer can provide a much higher PEC cathodic performance than pure TiO_2 nanolayer, in addition, it could provide a passivation protect for 316L SS without any light illumination (see Fig. 6-1). This work bring us the inspiration that more multifunctional PEC cathodic coatings can be developed to push this technique to practical application as soon as possible.

6.2. Spray pyrolysis technique

Spray pyrolysis technique is a quick and large-scale method for semiconductor thin film preparation. Ohko et al. [53] dispersed bis(2,4-pentanedionato)titanium oxide into the ethanol to get a precursor, and then sprayed it on the surface of 304 SS under a high temperature, to fabricate a TiO_2 covered layer on 304 SS. Fig. 6-2 presents that a compact TiO_2 thin film with a thickness 1.2 μm was covered on the surface of 304 SS. Further results showed that this TiO_2 thin film could provide −350 mV cathodic potential and a physical isolate protection to the 304 SS.

6.3. Liquid phase deposition technology

Liquid phase deposition is a more suitable method for large-scale TiO_2 thin film deposition on the metals under a low deposition temperature. Lei et al. [18] employed a simple liquid phase deposition method to prepared a TiO_2 thin film on the surface of 304 SS. The morphology of the thin film is shown in Fig. 2-3. However, the crystallinity of the TiO_2 thin film deposition by this method is not high enough, so for improving it, a subsequent high temperature anneal should be carried out, which would increase the complexity of this technique.

To date, mainly works focused on fabricate photoanode to PEC cathodic protection metals. This method is suitable used to protect these metals worked under water or ground where the sunlight can't arrive. However, actually, more metals are used in the atmosphere environment directly, so it is very important to develop overlayer PEC cathodic protection method in the future.

7. Outlook

At present, although the PEC cathodic protection technology shows a high potential for engineering applications, there are still some problems need to be solved.

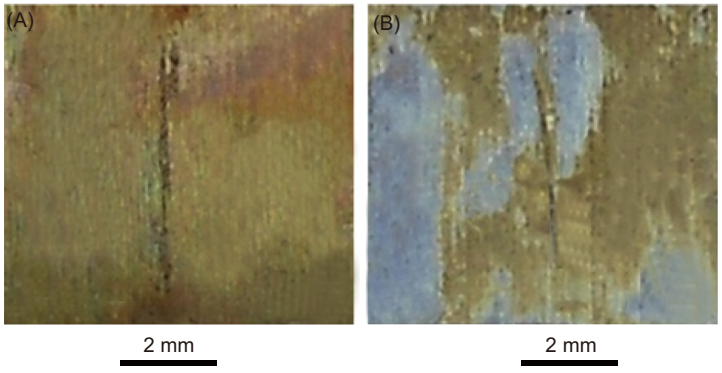

Fig. 6-1. Visual coating photographs after exposure to 2 M NaCl solution for 14 h at 60 °C: (A) pure TiO_2 coating, (B) 1% Cr–TiO_2 coating.

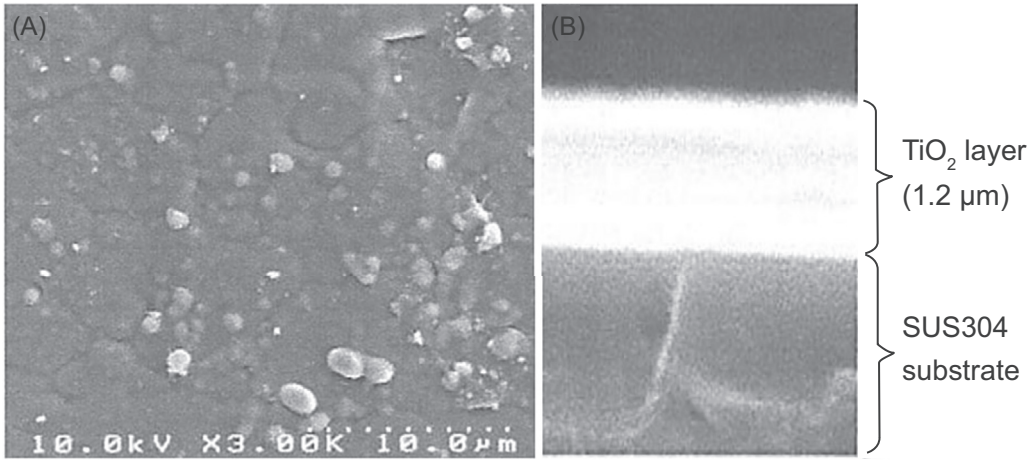

Fig. 6-2. SEMs of (A) the surface and (B) the cross section of SUS 304 coated with TiO_2 thin film.

7.1. Enhancing the photoinduced cathodic protection potential

Photoinduced cathodic protection potential is the most importance parameter for the metal cathodic protection. In general, when photogenerated electrons inject on a metal substrate, it is necessary to polarize the corrosion potential of the metal over 200 mV towards the cathode direction to achieve a considerable protection performance. Usually, a more negative CB potential of the semiconductor, more negative cathodic polarization potential for metal can be achieved. At present, the CB potential of widely used TiO_2 is near −0.29 V (vs NHE), it can just provide PEC cathodic protection for some stainless steels and copper with positive self-corrosion potential. However, it cannot provide PEC cathodic protection efficiency for some widely used and cheap metals, such as carbon steel and weathering steel. Thus, it is necessary to develop some n-type semiconductors with more negative CB potential to apply in this field. So far, $SrTiO_3$ (The CB potential is −0.49 V vs NHE) with negative CB potential has been studied, however, some other metal titanate semiconductors with more negative CB potential, such as $AlTiO_3$ (CB potential is −0.86 V vs NHE) and $MgTiO_3$ (CB potential is −0.75 V vs NHE) have not been researched, they are also some interesting PEC cathodic protection semiconductor materials. Although the CB potentials of the above three kinds of metal titanate semiconductors are negative enough, they can just stimulate by the ultraviolet light. Thus, it is necessary to form a suitable doping level at the top edge of the VB by energy band engineering, such as doping and alloying methods.

7.2. Improving the photoinduced photocurrent density of PEC cathodic protection materials

The photocurrent density of the PEC cathodic protection semiconductor thin films should be improved as well. On the condition of the photogenerated electrons can transfer to the protected metal, although the photocurrent can't decide the upper limit value of the PEC cathodic protection potential, it is believed that the value of the PEC cathodic protection potential is in direct proportion to the value of the photoinduced photocurrent within certain range. Especially for the PEC photoanode protection method, the photocurrent density of the photoanode is higher, the protected area of the metal is larger. In general, the photocurrent density of the photoanode can be improved by shortening the width of band gap, optimizing the transfer ratio of the electrons and decreasing the energy barrier of the surface electrochemical reaction. However, there are some special requirements on modification of photoanode materials who applied in PEC cathodic protection systems. For examples, during shorten the band gap width of one semiconductor, it is necessary to ensure that keep the CB potential negative enough and keep the band gap width higher than 2.6 eV.

Usually, combination of photoanode with some materials that possesses high conductivity, such as noble metals, carbon-based material and conductive polymer, can improve the charge transfer capacity that enhance the PEC performance of the photoanode for water splitting. However, for the PEC cathodic protection photoanode, some materials with too positive work function potential are not suitable to composite with it because the Fermi level potential of the semiconductor will be positive pulled that lowering the energy of the photogenerated electrons and decreasing the PEC cathodic protection potential of the photoanode. Furthermore, if the mass of compounded conductive material is too much, it will compete with the semiconductor during the photons absorption process, that decreasing the PEC performance of the photoanode. So, some conductive materials with negative work functions are more suitable for PEC cathodic protection photoanode modification, meanwhile, the mass of them should keep slight.

In addition, sensitizing the TiO_2 photoanode by some visible light response semiconductors is also a effective method to improve the PEC cathodic protection current density of it. Meanwhile, there is no work to discuss the long-term working stability about the sensitized-TiO_2 photoanode, but it is a very important to be made clear, because of the unstability property of the sensitizers. So, in the near future, some other sensitized semiconductors and some more interesting sensitized structure to enhance the stability of the photoande should be developed in this field [98–101].

After photogenerated electrons transfer to the metal, the holes on the surface of photoanode will oxidize the water to oxygen. This reaction is very important for the PEC cathodic protection process. If the water oxidation rate is very slow, the accumulated photogenerated holes will recombine with the electrons, that decreasing the PEC cathodic protection efficiency. Thus, reducing the surface water oxidation energy barrier is very emergency for PEC cathodic protection photoanode. Some water oxidation co-catalysts possess high potential for it performance improving.

7.3. Improving the photoelectrons storage capacity of the PEC cathodic protection system

Some materials with larger capacity for photogenerated electrons storage and negative enough discharge potential, can be applied in the field of PEC cathodic protection. So far, WO_3 and SnO_2 have been used in this field, but there are some problems about these materials such as low electronic storage ability and positive discharge potential. They cannot provide protection for some metals with negative self-corrosion potential after cutting off the light. Thus, it is necessary to develop some electron storage materials (such as Li_2TiO_3, CeO_2, Ployaniline etc.), whose discharge potential is negative enough and storage capacity big enough, to combine with the photoanode materials.

7.4. Combination of the PEC cathodic protection and traditional metal anticorrosion method

Sometimes, PEC cathodic protection can't provide a completely protect for metals, especially in the night and rainy weather. So, combination of the PEC cathodic protection method with other traditional metal anticorrosion method is very significant to improve the protection efficiency of metal.

Firstly, the PEC cathodic protection materials can cooperate with some metal surface passivative elements (such as Ni, Cr and B and P etc.). During we prepared semiconductor thin film on the metal, doping these metal passivative elements into the semiconductor, a difunction about this thin film can be achieved. For the one, the band gap width of the semiconductor can be narrowed by these elements doping. For the other one, in addition to provide PEC cathodic protection, this doped semiconductor can passivate the surface of the metal, to improve the anticorrosion performance for it further.

Secondly, composition the PEC cathodic protection semiconductor with the solid organic polymer corrosion inhibitor. Organic polymer corrosion inhibitors (such as polyethyleneimine, butyl acrylate and polyaniline etc.) have been widely used in the field of metal anticorrosion. So, these corrosion inhibitors can be employed to composite with the PEC cathodic protection semiconductor, to fabricate a PEC cathodic protection-corrosion inhibiting bifunction materials. There are many works should be done in this area, such as materials choosing, semiconductor surface modification for graft with organic polymer, design more suitable semiconductor-organic polymer interface for photogenerated charges exchange, increasing the stability of the organic polymer during PEC cathodic protection etc.

Except the mentioned above two combination ideas, furthermore crosses between PEC cathodic protection technology and traditional metal anticorrosion technology will be discovered in the future.

7.5. PEC cathodic protection coating technology

PEC cathodic protection technology is divided into two methods, including photoanode cathodic protection method and overlayer cathodic protection method. The formal one should fabricate a n-type semiconductor film on a conduction substrate (FTO, ITO, Ti etc.) to form a photoanode. Usually, this method was employed to protect the metals used under water or ground. Because the conduction substrates used to fabricate photoanode are chemical and thermal stable enough, a litter limits have been taken in during the photoanode fabrication process. Another advantage of this technology is that some holes sacrificial agents can be added in the photoanode cell, to increase the reaction rate of the anode process, thus it provides more free photogenerated electrons to cathodic protect the metal. There are two disadvantages about this method, firstly, the protection system is very complex, because a salt bridge and a counter electrode should be set between photoanode cell and corrosion cell. Secondly, the PEC photoanode protection method can't provide a surface physical protection of the metal, so the protection effective for metal is simplex.

PEC overlayer cathodic protection method requires to fabricate a semiconductor coating on the surface of protected metal, and this metal can be used under sunlight directly. Compared with PEC photoanode cathodic protection method, it means that except provide a PEC cathodic protection for the metal, the semiconductor overlayer can provide physical isolation protect for the metal also. In addition, some passivation elements or corrosion inhibitors can be added into this overlayer, to achieve a dual protection on the metal anticorrosion.

PEC overlayer cathodic protection is a more potential metal anticorrosion technology for practical application. Firstly, this surface semiconductor coating can be employed to protect metals in the air directly, that can simplify of the protection system. Secondly, the overlayer can absorb the sunlight in the atmosphere environment directly, that enlarge the application range of this technology. Lastly, it is possible to design a multifunction anticorrosion overlayer to protect the metal better. However, to date, just few works focus on this technology, meaning that this field has not caused widely attentions. Now it is believed that three potential problems should be researched in the near future: (1) Some physical characteristics of the semiconductor thin film such as the stickiness, mechanical strength and stability should be resolved further; (2) Sol−gel method is one of the most common method to prepare semiconductor thin film on metal. However, this thin film prepared by sol−gel method would be a avoidless mesoporous one, inducing by the organic removing during the annealing process. These mesoporous will decrease the physical isolation performance of the semiconductor thin film that decrease the anticorrosion capacity for protected metal. So some more thin film fabrication methods, such as magnetron sputtering, supersonic spraying and electrochemical deposition method and so on, should be developed to improve the quality of the semiconductor thin film; (3) To date, only TiO_2 has been developed and used in PEC overlayer cathodic protection field, it is very emergency to develop some different semiconductor thin films with more negative CB potential to protect the metals.

Conflict of interest

There is no conflict of interest.

Acknowledgment

The project was supported by National Natural Science Foundation of China (Grant no. 41506093).

References

[1] B.A. Shaw, R.G. Kelly, Electrochem. Soc. Interface (2006) 24−26.
[2] J. Ma, J. Wen, J. Alloys Compd. 496 (2010) 110−115.
[3] C. Christodoulou, G. Glass, J. Webb, S. Austin, C. Goodier, Corros. Sci. 52 (2010) 2671−2679.
[4] M.B. González, S.B. Saidman, Corros. Sci. 53 (2011) 276−282.
[5] Y. Ohko, S. Saitoh, T. Tatsuma, A. Fujishima, J. Electrochem. Soc. 148 (2001) B24−B28.
[6] H.W. Park, K.Y. Kim, W.Y. Choi, J. Phys. Chem. B 106 (2002) 4775−4781.
[7] R. Liu, Z. Zheng, J. Spurgeon, X. Yang, Energy Environ. Sci. 7 (2014) 2504−2517.
[8] Z. Zhang, J.T. Yates Jr., Chem. Rev. 112 (2012) 5520−5551.
[9] L. Song, X. Ma, Z. Chen, B. Hou, Corros. Sci. 87 (2014) 427−437.
[10] L. Song, Z. Chen, Corros. Sci. 86 (2014) 318−325.
[11] L. Song, Z. Chen, J. Electrochem. Soc. 162 (2015) C79−C84.

[12] M. Sun, Z. Chen, Y. Bu, J. Yu, B. Hou, Corros. Sci. 82 (2014) 77–84.
[13] A. Fujishima, K. Honda, Nature 238 (1972) 37–38.
[14] B. O'regan, M. Gratzel, Nature 353 (1991) 737–740.
[15] S. Rani, S.C. Roy, M. Paulose, O.K. Varghese, G.K. Mor, S. Kim, S. Yoriya, T.J. LaTempa, C.A. Grimes, Phys. Chem. Chem. Phys. 12 (2010) 2780–2800.
[16] M. Paulose, O.K. Varghese, G.K. Mor, C.A. Grimes, K.G. Ong, Nanotechnology 17 (2005) 398–402.
[17] J. Yuan, S. Tsujikawa, J. Electrochem. Soc. 142 (1995) 3444–3450.
[18] C.X. Lei, H. Zhou, Z.D. Feng, Y.F. Zhu, R.G. Du, Appl. Surf. Sci. 257 (2011) 7330–7334.
[19] C.X. Lei, H. Zhou, Z.D. Feng, J. Alloys. Compd. 542 (2012) 164–169.
[20] J. Li, C.J. Lin, C.G. Lin, J. Electrochem. Soc. 158 (2011) C55–C62.
[21] H. Yun, C.J. Lin, J. Li, J.R. Wang, H.B. Chen, Appl. Surf. Sci. 255 (2008) 2113–2117.
[22] M.C. Li, S.Z. Luo, P.F. Wu, J.N. Shen, Electrochim. Acta 50 (2005) 3401–3406.
[23] C.X. Lei, H. Zhou, C. Wang, Z.D. Feng, Electrochim. Acta 87 (2013) 245–249.
[24] Y.F. Zhu, R.G. Du, W. Chen, H.Q. Qi, C.J. Lin, Electrochem. Commun. 12 (2010) 1626–1629.
[25] G.X. Shen, Y.C. Chen, C.J. Lin, Thin Solid Films 489 (2005) 130–136.
[26] M.M. Sun, Z.Y. Chen, J.Q. Yu, Electrochim. Acta 109 (2013) 13–19.
[27] S.N. Li, J.J. Fu, Corros. Sci. 68 (2013) 101–110.
[28] S.N. Li, Q. Wang, T. Chen, Z.H. Zhou, Y. Wang, J.J. Fu, Nanoscale Res. Lett. 7 (2012) 1–10.
[29] Y. Liu, C. Xu, Z.D. Feng, Appl. Surf. Sci. 314 (2014) 392–399.
[30] J. Li, H. Yun, C.J. Lin, J. Electrochem. Soc. 154 (2007) C631–C636.
[31] J. Li, C.J. Lin, Y.K. Lai, R.G. Du, Surf. Coat. Technol. 205 (2010) 557–564.
[32] C.X. Lei, Z.D. Feng, H. Zhou, Electrochim. Acta 68 (2012) 134–140.
[33] J. Li, C.J. Lin, J.T. Li, Z.Q. Lin, Thin Solid Films 519 (2011) 5494–5502.
[34] Z.Q. Lin, Y.K. Lai, R.G. Hu, J. Li, R.G. Du, C.J. Lin, Electrochim. Acta 55 (2010) 8717–8723.
[35] H. Li, X.T. Wang, Y. Liu, B.R. Hou, Corros. Sci. 82 (2014) 145–153.
[36] R.H. Baughman, A.A. Zakhidov, W.A. de Heer, Science 297 (2002) 787–792.
[37] G. Jiang, Z. Lin, L. Zhu, Y. Ding, H. Tang, Carbon 48 (2010) 3369–3375.
[38] W. Liu, Y.G. Wang, G. Su, L.X. Cao, M.L. Sun, X.Q. Guo, H.M. Xu, R.J. Duan, Carbon 50 (2012) 3641–3648.
[39] X.Q. Guo, W. Liu, L.X. Cao, G. Su, H.M. Xu, B.H. Liu, Appl. Surf. Sci. 283 (2013) 498–504.
[40] C.X. Lei, Y. Liu, H. Zhou, Z.D. Feng, R.G. Du, Corros. Sci. 68 (2013) 214–222.
[41] J.G. Mavroides, J.A. Kafalas, D.F. Kolesar, Appl. Phys. Lett. 28 (1976) 241–243.
[42] M.S. Wrighton, P.T. Wolczanski, A.B. Ellis, J. Solid State Chem. 22 (1977) 17–29.
[43] S. Ahuja, T.R.N. Kutty, J. Photochem. Photobiol. A 97 (1996) 99–107.
[44] M. Matsumura, M. Hiramoto, H. Tsubomura, J. Electrochem. Soc. 130 (1983) 326–330.
[45] V. Subramanian, R.K. Roeder, E.E. Wolf, Ind. Eng. Chem. Res. 45 (2006) 2187–2193.
[46] Y. Liu, L. Xie, Y. Li, R. Yang, J.L. Qu, Y.Q. Li, X.G. Li, J. Power Sources 183 (2008) 701–707.
[47] H.R. Zhang, G.S. Miao, X.P. Ma, B. Wang, Int. J. Photoenergy 2013 (2013) 1–6.
[48] J. Poth, R. Haberkorn, H.P. Beck, J. Eur. Ceram. Soc. 20 (2000) 707–713.
[49] U.K.N. Din, T.H.T. Aziz, M.M. Salleh, A.A. Umar, Int. J. Miner., Metall. Mater. 23 (2016) 109–115.
[50] Y.Y. Bu, W.B. Li, J.Q. Yu, X.T. Wang, M.L. Qi, M.Y. Nie, B.H. Rong, Acta Phys. Chim. Sin. 27 (2011) 2393–2399.
[51] W. Fan, L. Niinistö, Mater. Res. Bull. 29 (1994) 451–458.
[52] Z.B. Jiao, T. Chen, J.Y. Xiong, T. Wang, G.X. Lu, J.X. Ye, Y.P. Bi, Sci. Rep. 3 (2013) 1–6.
[53] Y. Ohko, S. Saitoh, T. Tatsuma, A. Fujishima, Electrochem. Solid-State Lett. 5 (2002) B9–B12.
[54] H. Kato, A. Kudo, J. Phys. Chem. B 106 (2002) 5029–5034.
[55] J.W. Liu, G. Chen, Z.H. Li, Z.G. Zhang, J. Solid State Chem. 179 (2006) 3704–3708.
[56] S. Tonda, S. Kumar, O. Anjaneyulu, V. Shanker, Phys. Chem. Chem. Phys. 16 (2014) 23819–23828.
[57] D.F. Wang, J.H. Ye, T. Kako, T. Kimura, J. Phys. Chem. B 110 (2006) 15824–15830.
[58] S.X. Ouyang, H. Tong, N. Umezawa, J.Y. Cao, P. Li, Y.P. Bi, Y.J. Zhang, J.H. Ye, J. Am. Chem. Soc. 134 (2012) 1974–1977.
[59] R.B. Comes, P.V. Sushko, S.M. Heald, R.J. Colby, M.E. Bowden, S.A. Chambers, Chem. Mater. 26 (2014) 7073–7082.
[60] Q. Wang, T. Hisatomi, S.S.K. Ma, Y.B. Li, K. Domen, Chem. Mater. 26 (2014) 4144–4150.
[61] K. Iwashina, A. Kudo, J. Am. Chem. Soc. 133 (2011) 13272–13275.
[62] T.H. Xie, X.Y. Sun, J. Lin, J. Phys. Chem. C 112 (2008) 9753–9759.
[63] J.S. Wang, S. Yin, M. Komatsu, Q.W. Zhang, F. Saito, T. Sato, J. Photochem. Photobiol. A 165 (2004) 149–156.
[64] H. Yu, S.C. Yan, Z.S. Li, T. Yu, Z.G. Zou, Int. J. Hydrogen Energy 37 (2012) 12120–12127.
[65] T.P. Cao, Y.J. Li, C.H. Wang, C.L. Shao, Y.C. Liu, Langmuir 27 (2011) 2946–2952.
[66] S. Choudhary, A. Solanki, S. Upadhyay, N. Singh, V.R. Satsangi, R. Shrivastav, S. Dass, J. Solid State Electrochem. 17 (2013) 2531–2538.
[67] D. Sharma, A. Verma, V.R. Satsangi, R. Shrivastav, S. Dass, Int. J. Hydrogen Energy 39 (2014) 4189–4197.
[68] T. Tatsuma, S. Saitoh, Y. Ohko, A. Fujishima, Chem. Mater. 13 (2001) 2838–2842.
[69] R. Subasri, T. Shinohara, Electrochem. Commun. 5 (2003) 897–902.
[70] R. Subasri, S. Deshpande, S. Seal, T. Shinohara, Electrochem. Solid-State Lett. 9 (2006) B1–B4.
[71] M. Miyauchi, A. Nakajima, T. Watanabe, K. Hashimoto, Chem. Mater. 14 (2002) 2812–2816.
[72] J. Luo, P.A. Maggard, Adv. Mater. 18 (2006) 514–517.
[73] S. Burnside, J.E. Moser, K. Brooks, M. Gratzel, J. Phys. Chem. B 103 (1999) 9328–9332.
[74] Y. Zhang, Y.Y. Bu, J.Q. Yu, P. Li, J. Nanopart. Res. 15 (2013) 1–8.
[75] Y.F. Zhu, L. Xu, J. Hu, J. Zhang, R.G. Du, C.J. Lin, Electrochim. Acta 121 (2014) 361–368.
[76] Q.P. Luo, X.Y. Yu, B.X. Lei, H.Y. Chen, D.B. Kuang, C.Y. Su, J. Phys. Chem. C 116 (2012) 8111–8117.
[77] Z.B. Yu, Y.P. Xie, G. Liu, G.Q.M. Lu, X.L. Ma, H.M. Cheng, J. Mater. Chem. A 1 (2013) 2773–2776.
[78] C. Yu, K. Yang, Y. Xie, Q. Fan, C.Y. Jimmy, Q. Shu, C. Wang, Nanoscale 5 (2013) 2142–2151.
[79] J.X. Sun, Y.P. Yuan, L.G. Qiu, X. Jiang, A.J. Xie, Y.H. Shen, J.F. Zhu, Dalton Trans. 41 (2012) 6756–6763.
[80] W.W. He, H.K. Kim, W.G. Wamer, D. Melka, J.H. Callahan, J.J. Yin, J. Am. Chem. Soc. 136 (2013) 750–757.
[81] M.M. Sun, Z.Y. Chen, Y.Y. Bu, J.Q. Yu, B.R. Hou, Corros. Sci. 82 (2014) 77–84.
[82] J.P. Jing, Z.Y. Chen, Y.Y. Bu, Int. J. Electrochem. Sci. 10 (2015) 8783–8796.
[83] H.M. Xu, W. Liu, L.X. Cao, G. Su, R.J. Duan, Appl. Surf. Sci. 301 (2014) 508–514.
[84] X.C. Wang, K. Maeda, A. Thomas, K. Takanabe, G. Xin, J.M. Carlsson, K. Domen, M. Antonietti, Nat. Mater. 8 (2009) 76–80.
[85] S.C. Yan, Z.S. Li, Z.G. Zou, Langmuir 25 (2009) 10397–10401.
[86] Z.J. Huang, F.B. Li, B.F. Chen, T. Lu, Y. Yuan, G.Q. Yuan, Appl. Catal. B 136 (2013) 269–277.
[87] G.D. Ding, W.T. Wang, T. Jiang, B.X. Han, H.L. Fan, G.Y. Yang, ChemCatChem 5 (2013) 192–200.
[88] J.S. Zhang, X.F. Chen, K. Takanabe, K. Maeda, K. Domen, J.D. Epping, X.Z. Fu, M. Antonietti, X.C. Wang, Angew. Chem. Int. Ed. 49 (2010) 441–444.
[89] Y.Y. Bu, Z.Y. Chen, J.Q. Yu, W.B. Li, Electrochim. Acta 88 (2013) 294–300.
[90] Y.Y. Bu, Z.Y. Chen, RSC Adv. 4 (2014) 45397–45406.
[91] M.M. Sun, Z.Y. Chen, Y.Y. Bu, J. Alloys Compd. 618 (2015) 734–741.

[92] Y.Y. Bu, Z.Y. Chen, Electrochim. Acta 144 (2014) 42−49.
[93] T. Tatsuma, S. Saitoh, P. Ngaotrakanwiwat, Y. Ohko, A. Fujishima, Langmuir 18 (2002) 7777−7779.
[94] H. Park, A. Bak, T.H. Jeon, S. Kim, W. Choi, Appl. Catal. B 115 (2012) 74−80.
[95] P. Ngaotrakanwiwat, S. Saitoh, Y. Ohko, T. Tatsuma, A. Fujishima, J. Electrochem. Soc. 150 (2003) A1405−A1407.
[96] P. Ngaotrakanwiwat, T. Tatsuma, J. Electroanal. Chem. 573 (2004) 263−269.
[97] R. Subasri, T. Shinohara, K. Mori, Sci. Technol. Adv. Mater. 6 (2005) 501−507.
[98] Z. Xia, X. Zhou, J. Li, U. Qu, Sci. Bull. 60 (2015) 1395−1402.
[99] N. Lu, Y. Su, J. Li, H. Yu, X. Quan, Sci. Bull. 60 (2015) 1281−1286.
[100] C. Meng, Z. Liu, T. Zhang, J. Zhai, Green Chem. 17 (2015) 2764−2768.
[101] Z. Liu, Z. Hu, H. Huang, Q. Zhang, T. Zhang, J. Zhai, L. Jiang, J. Mater. Chem. 22 (2012) 22120−22125.